

Raiders of the Lost Mud: The geology behind drilling incidents within the Balder Formation around the Corona Ridge, West of Shetland

Douglas Watson¹, Nick Schofield^{1*}, Alistair Maguire², Christine Telford³, Niall Mark¹, Stuart Archer⁴, & Jonathon Hardman¹

¹ Department of Geology & Petroleum Geology, University of Aberdeen, Aberdeen, AB24 3UE, UK

² Schlumberger, Peregrine Road, Elrick, Westhill, AB32 6TJ, UK

³ CTC Geo Ltd, 176 Portland Road, Jesmond, Newcastle Upon Tyne, NE2 1DJ

⁴ MÆRSK OLIE OG GAS A/S, a Company of TOTAL, Amerika Plads 29, 2100 Copenhagen Ø, Denmark

* Correspondence: n.schofield@abdn.ac.uk

Abstract: The Faroe-Shetland Basin, NE Atlantic continental margin, hosts a number of important hydrocarbon fields, though deep water and narrow weather windows mean drilling costs are considerably higher than other parts of the UK Continental Shelf. Any additional drilling complications are therefore important to predict and negate as such issues can result in avoidable multi-million pound cost implications. This study focuses on the Corona Ridge, an intra-basinal high which contains the Rosebank Field, where a plethora of drilling issues, of enigmatic origin, are common within a key stratigraphic marker known as the Balder Formation. Drilling fluid loss, bit balling, wellbore breakouts, and wellbore “ballooning”, where lost drilling fluid returns to the wellbore, are all recognised within the Balder Formation along the Corona Ridge. We find that many of the drilling incidents can be traced back to both the lithological character of the Balder Formation, and the mid-Miocene tectonic inversion of the Corona Ridge. Moreover, we find that this geological explanation has wider implications for exploration in the region, including mitigation of drilling incidents in future wells through drill bit selection.

The Faroe-Shetland Basin, located on the NE Atlantic continental margin, represents one of the last remaining exploration frontiers of the UK Continental Shelf, with arguably the greatest remaining potential for significant new discoveries (Ellis & Stoker 2014; Austin *et al.* 2014). One particularly prospective area of the Faroe-Shetland Basin is the Corona Ridge (Fig. 1), an intra-basinal high which hosts a number of oil and gas discoveries, notably the ~240 million barrels of oil equivalent Rosebank Field (Austin *et al.* 2014). A challenging aspect of exploring around the Corona Ridge area, though, is high drilling costs associated with deep water (up to 1.5 km in places) and extreme weather conditions (Austin *et al.* 2014), necessitating the use of either fifth generation semi-submersible drill rigs (\$125,000/day) or dynamically positioned drillships (\$145,000/day) (IHS Markit 2018) in order to drill exploration and appraisal wells. Further exploration costs result from a myriad of drilling complications, particularly through thick volcanic sequences. Previous research has focused on drilling efficiency through these volcanic sequences, emphasising how key lithological properties contribute to

37 different drilling and well control issues (Archer *et al.* 2005; Millet *et al.* 2014; Millet *et al.* 2015; Millet
38 *et al.* 2016; Mark *et al.* 2018). However, a critical aspect of drilling operations around the Corona Ridge
39 that has been overlooked is drilling issues encountered within a volcanic unit in the uneconomic
40 overburden: specifically, the Balder Formation, an early Eocene aged unit consisting of interbedded
41 volcanic tuffs (lithified ash), claystone and siltstone (Watson *et al.* 2017). These drilling issues have
42 included drilling fluid loss, bit balling (clogging), borehole breakouts and wellbore “ballooning”, where
43 lost drilling fluid later returns to the wellbore. We propose that these drilling events can be linked
44 back to the regional geological history, particularly given their concentration along, or close to, the
45 Corona Ridge. By synthesising these findings with wider regional knowledge, we highlight that many
46 of the drilling issues can be traced back to the tectonic event that enhanced the Corona Ridge.
47 Furthermore, our findings have wider implications for future exploration in the region, including
48 suggestions for mitigation of drilling issues (leading to cost reduction) in future exploration wells, for
49 example through selecting a PDC drill bit as opposed to a tricone bit.

50

51 **Geological setting**

52 The Faroe-Shetland Basin (FSB) is located along the NE Atlantic continental margin, situated between
53 the Faroe Islands and the Shetland Islands (Fig. 1). The FSB is a series of SW-NE trending sub-basins,
54 formed through multiple phases of Palaeozoic to Cenozoic rifting (Ritchie *et al.* 2011). These sub-
55 basins are delineated by intra-basinal highs of Precambrian crystalline basement capped by Mesozoic
56 sediments (Lamers & Carmichael 1999). During the Palaeocene to early Eocene the FSB was
57 characterised by widespread volcanism, associated with the presence of a mantle plume and the
58 commencement of rifting and crustal thinning between Greenland and NW Europe (White &
59 McKenzie 1989; Schofield *et al.* 2015; Hardman *et al.* 2018a). Later, during Eocene-Miocene times, the
60 FSB experienced several punctuated phases of compression, resulting in large scale inversion of the
61 intra-basinal highs, and the formation of elongate anticlines with four-way closure at Cretaceous-
62 Cenozoic level (Boldreel & Andersen 1993; Dore *et al.* 2008; Ritchie *et al.* 2008; Holford *et al.* 2009;

63 Holford *et al.* 2016). This study adopts the lithostratigraphy of Ritchie *et al.* (2011) and Stoker &
64 Varming (2011) (Fig. 2).

65

66 **Corona Ridge exploration history**

67 The FSB has been the focus of petroleum exploration since the 1970s. The basin hosts the prolific
68 Kimmeridge Clay marine source rock, thought to be responsible for sourcing the majority of the
69 hydrocarbons discovered in the region (Scotchman *et al.* 2006; Scotchman *et al.* 2016). A number of
70 hydrocarbon fields are present throughout the basin, generally overlying or close to intra-basinal highs
71 (Fig. 1a). This study concerns the Corona Ridge, an intra-basinal high located in the centre of the basin
72 (Fig. 1b). Figure 3 shows a seismic line cross-section running parallel through the Corona Ridge,
73 depicting the location of wells and structures examined in this study; the details of the seismic line can
74 be found in the methodology section of this work.

75 The first well located along the Corona Ridge was drilled in 1998 and tested the Eribol Prospect
76 (well 213/23-1), which encountered oil shows within Lower-Middle Carboniferous sandstones. The
77 Tobermory prospect (214/4-1), drilled in 1999, marked the first discovery of sizeable quantities of
78 hydrocarbons, when it encountered dry gas in Mid-Eocene turbidite fan sandstones. In the year 2000
79 the Bunnehaven exploration well (214/9-1, 17 km south of Tobermory) encountered oil (and
80 associated gas) within Palaeocene-Eocene fluvial-deltaic sandstones in addition to gas in Upper
81 Cretaceous marine sandstones. At present Bunnehaven and Tobermory are undeveloped, being
82 classed as uneconomic (as of 2018), though further nearby exploration (e.g. Lyon Prospect to be drilled
83 in 2019; Siccar Point Energy 2018) may lead to an economic cluster of gas fields in the north of the
84 FSB.

85 In 2004, 140 km southwest of Bunnehaven, the Chevron exploration well 213/27-1 encountered
86 oil and associated gas within Palaeocene-Eocene sandstones present between basalt lava flows
87 (Rosebank prospect), and oil within Upper Jurassic sandstones (Lochnagar prospect) (Duncan *et al.*
88 2009; Helland-Hansen 2009; Schofield & Jolley, 2013; Poppit *et al.* 2016; Hardman *et al.* 2018b). A
89 further six wells, two exploration and four appraisal, have established the extent of the Rosebank

90 Field, though has yet to be developed; Lochnagar is planned to remain undeveloped (Poppit *et al.* 2016).
 91 Later North Uist (213/25c-1), drilled in 2012, encountered significant gas shows above background
 92 within the Balder Fm., the Kimmeridge Clay and the Carboniferous. Finally well 6104/25-1, drilled in
 93 2014 within the Faroese sector, encountered only water-bearing sediments, within the Early Eocene
 94 Colsay (Sula prospect) and Hildasay targets (Stelkur prospect). In terms of trapping mechanisms,
 95 generally the Palaeocene-Eocene plays along the Corona Ridge, such as Rosebank, rely on inversion-
 96 induced anticlines. Meanwhile, older Mesozoic plays, principally the Jurassic, are hosted within tilted
 97 fault blocks sealed by Cretaceous mudstones (Duncan *et al.* 2009) (Fig. 3).

98 Within several of the wells drilled along the Corona Ridge, however, a variety of drilling issues are
 99 recorded within the Balder Formation (see text boxes in Fig. 3), which in practical terms forms part
 100 of the overburden. The cause of these drilling issues, which this study investigates, is currently
 101 unknown, and have a significant cost implication given that future exploration wells near Bunnehaven
 102 and the potential development wells of the Rosebank Field, will both have to drill through the Balder
 103 Formation to reach intended targets.

104

105 **Data and Methodology**

106 The main dataset used for this study is the released commercial borehole data from wells drilled in
 107 the UK Continental Shelf, from the Common Data Access (CDA). The wells used as case studies are
 108 listed in Table I. For consistency with previous work (Mark *et al.* 2018), a table detailing definitions of
 109 the terminology adopted by the offshore exploration and drilling industry is provided (supplementary
 110 material). Several seismic lines are also exhibited in this study, which are from the regional Faroese-
 111 Shetland PGS MegaSurvey Plus 3D seismic dataset, to place the wells examined in a tectono-
 112 stratigraphic context.

Well	Prospect/ Field name	Year Drilled	Balder depth [m MDBRT] (& Calculated Thickness [m])	Drilling fluid	Drill bit through Balder	Issues/notes within the Balder
------	-------------------------	-----------------	--	-------------------	--------------------------------	--------------------------------------

205/1-1	Rosebank (Main)	2007	2472-2537 (55)	WBM	PDC	None
213/26-1*	Rosebank (Main)	2007	2448-2514 (66)	WBM	Tricone	Drilling fluid loss
213/27-1*	Rosebank (Main)/ Lochnagar	2004	2395-2465 (70.5)	WBM	Tricone	Drilling Fluid loss
213/27-2	Rosebank (Main)	2007	2471-2532 (56)	WBM	PDC	Cement loss during liner placement
6104/25-1	Sula/Stelkur	2014	2471-2535 (63.5)	WBM	Hybrid	Drilling fluid losses and break-outs
213/27-3	Rosebank (North)	2008	2440-2471 (43.7)	WBM	PDC	None
213/23-1	Eribol	1998	2644-2677 (32.3)	WBM	Tricone	LOT- weak formation
213/25c-1*	North Uist	2012	3017-3076 [†] (69.1)	WBM & OBM [‡]	Tricone	Fluid losses, hole collapse, BHA lost in hole
214/27-1	Flett Ridge	1985	2301-2367 (67.1)	WBM	Tricone	Cement loss during casing
214/9-1	Bunnehaven	2000	3524-3726 (189)	WBM	Tricone	Drilling fluid loss & ballooning.
214/4-1	Tobermory	1999	3456-3734 (80)	WBM	Tricone	Drilling fluid losses & pack offs

113 **Table 1:** List of well case studies from south to north within the FSB. Note the drilling parameters,
114 which will be referred to in the results section of this work. Depths are in Measured Depth Below
115 Rotray Table (MDBRT). * = includes sidetracks. † = base depth projected from deviated sidetrack.
116 WBM = water based mud, which in each instance is a KCl polymer. ‡ = OBM, Oil-based mud, used in

117 final side-track where no drilling issues recorded. PDC = Polycrystalline diamond compact, a type of drill
118 bit. BHA = Bottom Hole Assembly. LOT = Leak Off Test.

119 ***Character and identification of the Balder Formation***

120 The Balder Formation is an early Eocene lithostratigraphic unit, characterised by an interbedded
121 assemblage of siltstone, claystone, and volcanic tuffs (lithified ash) (Knox & Holloway 1992; Mudge
122 2014; Watson *et al.* 2017). During burial the volcanic tuffs are almost entirely altered to smectitic or
123 bentonitic clays (Knox & Morton 1983; Malm *et al.* 1984; Knox & Morton 1988). As a consequence of
124 the original volcanic component, the Balder Formation has a prominent well log character (Fig. 4),
125 manifested as low gamma akin to sandstone (Fig. 4a), resistivity moderately higher than shale (4b), a
126 density/neutron positive separation of a shale (4c), and a fast interval transit time that has a bell-shaped
127 log signature (4d) (Watson *et al.* 2017). The Balder Formation is also laterally extensive and a
128 prominent seismic marker (due to a marked acoustic impedance contrast with the surrounding
129 claystones).

130

131 ***Drilling the Balder Formation***

132 A major focus of this study is drilling behaviour through the Balder Formation, which is best
133 understood in the context of the drilling window (Fig. 5). The drilling window is a wellbore pressure
134 profile governing safe drilling, bounded on the lower limit by pore pressure, and the fracture pressure
135 on the upper limit (Cook *et al.* 2011). The wellbore pressure profile is represented by the mud
136 pressure, governed by the weight of the drilling fluid (expressed in pounds per gallon [ppg]) (Cook *et*
137 *al.* 2011). When examining drilling issues recorded within the Balder Formation, we either utilised a
138 pre-existing drilling window (present in end of well reports), or constructed our own, to help establish
139 the cause of particular drilling problems.

140 Pore pressure is the pressure exerted by the fluids within the rock and represents the lower
141 limit of the drilling window (Osborne & Swarbrick 1997). If the mud pressure is set too low, below
142 the pore pressure, then there is a danger of an unwanted influx of fluid from the wellbore, known as
143 a “kick” (Cook *et al.* 2011). The most reliable way to determine pore pressure is from Wireline

144 Formation Tester (WFT) data, where pressures are measured from the formation directly downhole
145 (Rider & Kennedy 2011). Marked increases in rates of penetration (ROP), known as “drilling breaks”,
146 are also helpful in highlighting potential zones of overpressure (Ablard *et al.* 2012).

147 The fracture pressure, the upper limit of the drilling window, represents the mud pressure
148 above which the tensile strength of the rock is exceeded causing failure and hydraulic fracturing of the
149 formation (Osborne & Swarbrick 1997; Cook *et al.* 2011; Millet *et al.* 2016). A consequence of
150 unintentionally fracturing the formation can be the loss of drilling fluid, which is both costly (as mud is
151 often on loan to the operator of a well), and unsafe as the wellbore pressure may drop, leading to loss
152 of the pressure barrier and the influx of formation fluid (i.e. a kick). In order to establish the fracture
153 pressure a Formation Integrity Test (FIT) or Leak-off Test (LOT) is performed at the start of each
154 new section of a well. A LOT is where the well is shut in, and a surface pressure is applied on top of
155 the pressure of the drilling mud column. The surface pressure is increased gradually until the pressure
156 is sufficiently high to fracture the formation, causing *leaking off* of drilling fluid. If the test is stopped
157 before fracturing then it is an FIT, providing an upper limit for the mud weight (the Equivalent
158 Circulating Density [ECD]) used when drilling the next section (Gaarenstroom *et al.* 1993).

159

160 ***Drill bits and drilling fluids***

161 Drilling issues which occur through the Balder Formation occur in some wells (e.g. 213/26-1) but not
162 in others (e.g. 205/1-1), even when in relatively close proximity (both examples within Rosebank Main),
163 suggesting that drilling parameters play a crucial role in operational complications. Two important
164 drilling variables between different wells, outwith of the geology, is the type of drill bit and type of
165 drilling fluid used. Drill bit selection is a critical pre-drill consideration as different bits perform more
166 effectively in different lithologies. The two most common drill bit types are (1) roller cone bits and (2)
167 fixed cutter bits. *Roller cone* bits (Fig. 6a) consist of three (a tricone bit) or four cone shaped steel
168 noses that turn on the rock surface at the bottom of the wellbore as the bit rotates. *Fixed cutters* (Fig.
169 6b) consist of a single head that rotates with no separately moving parts (Schlumberger 2018), chipping

170 and cutting away at the rock surface. A third, less common drill bit variant is a *hybrid drill bit* (Fig. 6c),
171 which consists of a fixed head cutter and 2 or 3 roller cones.

172 Roller cone bits are predominantly used to drill mixed successions of soft (e.g. coal and shale)
173 and moderately hard lithologies (such as sandstone and limestone) (Warren 1987). Fixed cutter bits,
174 such as Polycrystalline Diamond Compacts (PDC), are typically more expensive than roller cones,
175 though have more durable wear and therefore are more effective in very hard and abrasive formations
176 such as chert (German *et al.* 2015) and crystalline volcanic rocks (Grindhaug 2012). Hybrid bits are
177 used to drill an interbedded succession of very hard (e.g. basalt) and markedly softer rocks (e.g.
178 claystone) (Rickard *et al.* 2014). Of note within the separate drill bits utilised, are the location of the
179 nozzles, which pump out the drilling fluid at the front of the drill bit, in a similar fashion to the nozzle
180 on a garden hose. In both roller cone and hybrid drill bits, the nozzles tend to be located above and
181 slightly to the side of the main cutting cones, whereas the nozzles in a fixed cutter bit are more
182 centrally located and closer to the cutting surface (Fig. 6).

183 In terms of drilling fluids, the most common types used are water-based mud (WBM) and oil-
184 based mud (OBM). OBM provides greater wellbore stability, as clay bearing formations can interact
185 with WBM and cause swelling and ultimately formation damage (McLean & Addis 1990). In terms of
186 drilling in the UK Continental Shelf, OBM is generally reserved for drilling reservoir intervals.
187 Additives, such as potassium chloride (KCl) are often added to WBM in order to inhibit clays from
188 swelling (Caenn & Chillingar 1996).

189

190 **Results: Drilling characteristics of the Balder Formation around the Corona Ridge area**

191 ***Geomechanical properties***

192 An important initial step in determining the cause of drilling issues within the Balder Formation is to
193 establish its drilling window parameters; chiefly, what the pore pressure and fracture gradient of the
194 formation is across the Corona Ridge, and what mud weight was used to drill through the formation
195 in each well.

196 Any evidence of overpressure, i.e. pore fluid pressures in excess of hydrostatic pressure at a
197 specific depth (Osborne & Swarbrick 1997; Zoback 2010), is important to recognise as it is linked to
198 a number of drilling incidents, such as kicks and drilling fluid losses, which have been historically
199 encountered in wells in the FSB (Mark *et al.* 2018). There is, however, a lack of WFT data within the
200 Balder Formation as the lithologies such as tuffs and claystones present have permeability too low to
201 be measured with conventional WFTs. We therefore examined WFT data acquired from a variety of
202 formations throughout the Corona Ridge, in order to establish the study area pore pressure profile
203 around the depths at which the Balder Formation is intersected. When plotted, these WFT points
204 indicate that the depth zone at which the Balder Formation is encountered around the Corona Ridge
205 is normally pressured (e.g. Fig. 5), that is, it follows a normal hydrostatic gradient that would be
206 anticipated for pore connection up to the seabed. However, low permeability Palaeogene-aged shales
207 globally commonly exhibit overpressure beyond depths of 1500 m (Swarbrick & Osborne 1998).

208 There is also a scarcity of FIT and LOT data, the most reliable way to determine fracture
209 gradients, within the Balder Formation in the FSB, owing to the fact casing points are rarely set within
210 the Balder Formation itself. In this study we therefore examined a number of individual LOTs acquired
211 within the Balder Formation from five wells within the FSB and a further 7 wells from the contiguous
212 North Sea Basin; the latter of which hosts the Balder Formation and is lithologically similar to the FSB
213 (Mudge 2014; Watson *et al.* 2017). When plotting these LOT points (Fig. 7), the fracture gradient
214 measured within the Balder Formation displays a gradual increase with depth, as would be expected.
215 The fracture pressure measured along the Corona Ridge, acquired within the Balder from the Eribol
216 well (213/23-1), represents a marginal departure from this trend line, hydraulically fracturing 274 psi
217 (1.9 MPa) lower than the fracture gradient projected from the regional trend.

218

219 ***Drilling phenomena which occur within the Balder Formation***

220 There is a variety of drilling problems recorded through the Balder Formation around the Corona
221 Ridge, such as bit balling (clogging up of the bit) and drilling fluid losses, which contribute to non-
222 productive time (NPT) for drilling activity and even necessitate pulling out of the hole (POOH), at

223 great cost to troubleshoot and solve the problem. One “trip”, the process of pulling the drill string
224 out of the hole, can take up to 24 hours to complete, equating to \$125,000 in cost at the current
225 semi-submersible drill rig daily rate (IHS Markit 2018). The following section details specific drilling
226 issues encountered within the Balder Formation around the Corona Ridge, though with particular
227 emphasis on the Rosebank wells, all of which were drilled within the last 15 years and therefore have
228 a good selection of publicly available data, including drilling mechanics logs and wellbore image logs,
229 with which to investigate the nature and cause of drilling problems. In the southern part of Rosebank
230 Main (e.g. 213/26-1z) these drilling incidents typically occur within narrow ranges (~20 m) (Fig. 8).

231

232 *Bit Balling*

233 The initial drilling issue to occur in this narrow, 20 m depth range through the Balder Formation is bit
234 balling, which is when the formation interacts with the drilling fluid, and then proceeds to swell and
235 stick to the drill bit (Fig. 9) (Cheatham & Nahm 1990). Bit balling can significantly reduce rates of
236 penetration (ROP), preventing the drill bit from contacting the formation, and the built up mass of clay
237 can make the bottom hole assembly behave like a piston in a cylinder, producing additional surge and
238 swab pressures (Hariharan & Azar 1996). Unless balling is treated downhole, it may require pulling
239 out of the hole (POOH) to clean the drill bit, resulting in non-productive drilling time.

240 Bit balling is noted in drilling reports throughout Rosebank Main (213/26-1, 213/26-1z &
241 213/27-1z) and in the Bunnehaven (214/9-1) well. In Rosebank Main well 213/27-1z, bit balling was
242 recognised through the Balder Formation as ROP dropped to <1 m/hour at 2417.7 m measured depth,
243 after only the top 20 meters of the Balder Formation having been drilled. Forty-Five barrels (6,120
244 litres) equivalent worth of caustic material and seawater was put down the hole, in an attempt to
245 breakdown the build-up of swelling materials. However, the unballing strategy was unsuccessful and
246 eventually required POOH to clean the drill bit, resulting in approximately 24 hours of NPT. Taken
247 as a proportion of the £14.09 million total well cost of 213/27-1z, drilled over 51.6 days, cleaning of
248 the bit due to balling equates to a cost of £273,062 (1.94% of the entire well cost). A full suite of
249 drilling mechanics logs is not available for well 213/27-1z. However, drilling mechanics logs are available

250 for well 213/26-1z (Rosebank Main), drilled three years later, where balling was again encountered
251 within the Balder Formation. Within the drilling mechanics logs, balling causes a reduction in the rate
252 of penetration (ROP) (Fig. 8a), despite the weight on bit (WOB) being increased (Fig. 8b). Significantly,
253 the balling is concomitant with a gradual increase in standpipe pressure (Fig. 8c) (which represents
254 pressure in the circulating drilling fluid system), which eventually spikes (at 2582 psi), just prior to the
255 commencement of drilling fluid losses (Fig. 8d).

256

257 *Drilling fluid losses and gains (ballooning)*

258 In the narrow, 20 m depth range in 213/26-1z within the Balder Formation, dynamic drilling fluid loss
259 (losses as the drilling fluid is circulating during drilling) occurs immediately after the spike in standpipe
260 pressure associated with bit balling (Fig. 8c&d). Fluid losses also occur further down in the Balder and
261 in total occur in three separate zones (149 bbl/hr at 2522.8 m; 90 bbl/hr at 2529 m; 298 bbl/hr at
262 2575.6 m) (Fig. 8), categorising them as moderate, minor and severe losses, respectively (Millet *et al.*
263 2016). In an attempt to “cure” the losses, 110 barrels (14,960 litres) of Lost Circulation Material (LCM)
264 was pumped down the hole to plug the permeable zones. However, the resulting reduction in mud
265 supplies, in combination with a deteriorating weather forecast, resulted in POOH. During the
266 subsequent bad weather, 100 hours of NPT were ultimately accrued before the recommencement of
267 drilling; when taken as a proportion of the 57 days taken to drill 213/26-1z, this equates to £1.16
268 million. Including sidetracks, drilling fluid loss is recorded within the Balder Formation in six out of the
269 eleven wells (54.5 %) along the Corona Ridge: in 6104/25-1 (Sula/Stelkur), in 213/26-1 & 213/27-1
270 (Rosebank Main), North Uist (213/25-1c), Tobermory (214/4-1) and in Bunnehaven (214/9-1). In total,
271 more than 550 barrels (74,800 litres) of drilling fluid have been lost to the Balder Formation in these
272 Corona Ridge wells, equating to ~ £25,300 cost for just the mud alone.

273 Within three of these Corona Ridge wells which encountered drilling fluid losses through the
274 Balder Formation (213/26-1, Rosebank Main; 214/4-1, Tobermory; 214/9-1, Bunnehaven), the lost
275 drilling fluid later returned to the wellbore in a process called wellbore ballooning (Helstrup *et al.*
276 2004). Ballooning can be problematic as returning drilling fluid can be interpreted wrongly as an influx

277 of formation fluid (known as a “kick”). In the case of misinterpretation as a kick, consequently mud
278 weights may be increased to compensate for this influx, with the inadvertent effect of fracturing the
279 formation, and exacerbating drilling fluid loss (Helstrup *et al.* 2004; York *et al.* 2009). During
280 connections (the process of adding more pipe to the drillstring) circulation of the drilling mud is
281 stopped, and only the pressure of the static mud column holds back formation fluids from entering
282 the wellbore, which includes any lost drilling mud. Ballooning can therefore occur as the pressure of
283 the static mud column can be lower than the pressure of the lost drilling mud within the formation
284 (Ward & Clark 1998).

285

286 *Drilling Fractures*

287 The Balder Formation is characterised from mud logs as a series of low permeability interbedded
288 mudstone, siltstone and volcanic tuffs in wells around the Corona Ridge. Drilling fluid losses within
289 the Balder Formation therefore appear to be linked to several sets of electrically conductive fractures
290 recognised within Rosebank Main, specifically 213/26-1 and its sidetrack 213/26-1z where losses
291 occurred through the Balder. In well 213/26-1 these fractures appear as thin, electrically conductive
292 fractures sub-parallel with the wellbore, 180° apart (Fig. 10a), characteristic of drilling induced fractures
293 (Zoback *et al.* 2003). In well 213/26-1z, a more complex fracture pattern is recognised, with “one
294 winged” drilling induced, or at least enhanced, fractures (i.e. a single sub-parallel fracture with no pair)
295 (Fig. 10b) (Barton *et al.* 1995; Jepson *et al.* 2018) and several smaller fracture splays exhibiting an
296 irregular, dendritic pattern.

297 The fractures within 213/26-1 are typical of drilling induced fractures, though the fracture
298 network within 213/26-1z is more complex to characterise. One way to determine whether the
299 fractures within 213/26-1z are natural, i.e. pre-existing before drilling, is to examine whether
300 background gas increases in that interval, which is otherwise impossible with drilling induced fractures
301 (Rider & Kennedy 2011). Drilling fluid losses can complicate gas readings whilst drilling, though in
302 213/26-1z electrically conductive fractures are also observed deeper, where no drilling fluid losses
303 occurred. Between 2522-2525 m, where the fractures are located, methane levels increase from 1000

304 ppm at 2522 m, to 1900 ppm at 2525 m. Smaller pre-existing fractures are also recognised in well
305 205/1-1 in Rosebank Main (Fig. 10c) where the Balder Formation was drilled incident free. These
306 fractures are also associated with a small increase in background gas (methane increases from 4000
307 ppm at 2514 m, to 7000 ppm at 2515 m), suggesting they are, at least in part, pre-existing, fractures
308 that have been drilling enhanced (Rider & Kennedy 2011). Ultimately, there appears to be both drilling
309 induced and enhanced fractures in wells where losses occur (213/26-1 & 213/26-1z), and smaller pre-
310 existing fractures in wells where no drilling incidents were observed (e.g. 205/1-1).

311 Drilling induced and enhanced fractures also provide important evidence of regional stress,
312 and hence their underlying tectonic origin, which has important economic implications given that these
313 fractures are associated with costly drilling fluid losses. Fracture enlargement, including induced and
314 enhanced fractures, forms parallel to contemporary maximum horizontal stress (S_{Hmax}) (Fig. 11) (Dart
315 & Zoback 1989; Hillis & Williams 1992). The drilling induced (213/26-1) and drilling enhanced fractures
316 (213/26-1z) within the Balder Formation overlying the Corona Ridge are orientated NW-SE (Fig. 10a)
317 and NNW-SSE (Fig. 10b), respectively, approximately parallel with the predominant present day stress
318 field of WNW-SSE (Holford *et al.* 2016).

319 Unfortunately, drilling mechanics logs, including mud weights, are not available for well 213/26-
320 1, though are available from the sidetrack 213/26-1z. An unusual aspect of the drilling induced and/or
321 enhanced fractures within 213/26-1z is that the mud weight used (ECD of ~2407 psi) does not appear
322 to have exceeded the fracture gradient of the Balder Formation around the Corona Ridge (~2539 psi)
323 (Fig. 8).

324

325 Discussion

326 *Synthesising geology and drilling data - why the drilling issues occur*

327 In this study we have outlined how a number of drilling incidents encountered within the Balder
328 Formation occur in a narrow, ~20m depth range (e.g. Fig. 8). Image logs from Rosebank Main (Fig. 10)
329 highlight that within this zone there are large conductive fractures, up to 15 m long, interpreted as
330 either drilling induced (213/26-1) or enhanced (213/26-1z), which likely represent the source of

331 permeability by which the drilling fluid escapes from the wellbore. However, the mud pressure does
332 not appear to have exceeded the modelled fracture gradient of the Balder Formation, suggesting an
333 alternative mechanism for hydraulically fracturing the Balder is in effect.

334 Notably, examination of the standpipe pressure (pressure in the drilling fluid system) can be
335 seen to markedly increase from background readings, spiking just prior to occurrence of loss of drilling
336 fluid. When plotted, the pressure combination of mud pressure (ECD) and the excess in standpipe
337 pressure exceeds the modelled fracture pressure of the Balder (Fig. 12). Operationally, this is
338 interpreted as the bit balling creating a restricted flow, causing a spike in mud pressure which reaches
339 the fracture pressure, leading to drilling induced or enhanced fractures. We therefore suggest that the
340 drilling issues- including bit balling, drilling induced/enhanced fracturing, drilling fluid losses and
341 ballooning- occur in an inter-related chain reaction (visually depicted in Fig. 13) and detailed below:

342

- 343 1. Normal drilling conditions within the Balder Formation, no operational issues initially.
- 344 2. Balder Formation clays start to swell, causing balling of the drill bit and leading to a
345 reduction in ROP. An increase in WOB likely exacerbates this effect (akin to a car
346 continuing to accelerate wheels stuck in mud). Tricone and hybrid bits are more adversely
347 affected by this balling, as their drilling nozzles are located at the side of the bit and are
348 therefore less effective at clearing away the build-up of clay material.
- 349 3. The swelling clays cause restriction of flow, preventing communication between the area
350 in front of the drill bit (where the cuttings are being generated) to the rest of the wellbore
351 (termed a “pack-off”). When the well packs off the trapped pressure causes the formation
352 below the pack-off to be subject to higher pressure than calculated by mud weight and
353 ECD, to the point where the natural fractures within the Balder are enhanced. Drilling
354 fluid is then lost to those fractures.
- 355 4. The drilling fluid losses are “cured” by putting Lost Circulation Material (LCM) pills
356 pumped down the hole, plugging the facture network and allowing drilling to recommence.

357 5. The lost fluid later returns to the wellbore (ballooning), often during drill pipe connections
358 as only the static mud column is holding back formation fluids (which includes lost drilling
359 mud).

360

361 **Wider geological context- Why drilling issues occur around the Corona Ridge**

362 In this study we have detailed a range of drilling incidents observed within the Balder Formation around
363 the Corona Ridge area of the FSB. There are two critical features of the Balder Formation observed
364 in these wells: the formation is both (1) highly swelling and (2) a NW-SE principal stress orientation.

365 The swelling aspect can clearly be linked back to the lithological character of the Balder
366 Formation, particularly the volcanic tuffs which are now largely altered to smectite (Knox & Morton
367 1983), a clay type particularly prone to swelling (Norrish 1954; Cheatham & Nahm 1990). An
368 important aspect of the Balder Formation tuffs is that their distribution is regionally variable,
369 particularly when associated with marginal to non-marine deposition compared to marine settings
370 (Watson *et al.* 2017). In marginal to non-marine settings (Fig. 14), such as the southern (e.g. quads 204,
371 205) and eastern (e.g. Rona Ridge) flanks of the basin, tuff preservation is more limited, appearing
372 within discontinuous, relatively thin (2-12 m thick) packages. In marine settings such as the Flett Sub-
373 basin and the Corona Ridge, in contrast, tuffs are better preserved within predominantly siltstone and
374 claystone rich successions.

375 The drilling induced and enhanced fractures recognised within the Balder Formation along the
376 Corona Ridge document a principal horizontal stress orientated NW-SE. This orientation is parallel
377 with the dominant horizontal stress within the basin (Holford *et al.* 2016), and also coincident with
378 the orientation of Miocene-aged North Atlantic ridge-push compression, a postulated mechanism for
379 the inversion of SW-NE trending anticlines such as those overlying the Corona Ridge (Boldreel &
380 Andersen 1993; Ritchie *et al.* 2008). We therefore propose that the compression event that caused
381 inversion of the Corona Ridge lead to horizontal stresses sufficient to induce brittle deformation within
382 the Balder Formation, manifested as a fracture network that is later enhanced during the drilling
383 process.

384 Therefore, specifically in the case of the Corona Ridge, it appears that the combination of (1)
 385 marine Balder Formation with tuffs that are susceptible to swelling during drilling and (2) a mechanically
 386 weak Balder Formation subjected to NW-SE horizontal stress overlying intra-basinal highs, result in
 387 drilling issues related to the opening of pre-existing fractures (Fig. 14). To the south-west of Rosebank,
 388 wells around the Cambo intra-basinal high (e.g. Cambo Field) have not experienced drilling issues
 389 through the Balder Formation likely due to Cambo's closer proximity to the Balder palaeocoastline
 390 (Hardman *et al.* 2018a) and therefore more marginal marine sedimentation (greater proportion of
 391 non-tuffaceous siltstone and sandstone less prone to swelling).

392

393 **Mitigation against drilling issues for future wells**

394 Issues related to drilling through the Balder Formation around the Corona Ridge have led to
 395 a number of highly undesirable operational events, such as reduced ROP and loss of drilling fluid.
 396 Cumulatively, in total >550 barrels (74,800 litres) of drilling fluid have been lost, and at least 124 hours
 397 of NPT have been accrued, whilst drilling the Balder Formation around the Corona Ridge, which
 398 equates to approximately £1.5 million in cost. Therefore any mitigations which can be put in place to
 399 minimise drilling issues within the Balder Formation have a significant efficiency and monetary
 400 implication. Table 2 summarises a number of mitigations to prevent drilling issues through the Balder,
 401 addressed in further detail below.

Operation Mitigations	Selection	Impact
Mud type	Oil-based mud (OBM)	No reaction with swelling clays.
Bit choice	PDC bit	PDC bit nozzles more centrally located, likely more effective at clearing away build-up of swelling clays.
Mud pressure	Reduced mud pressure through the Balder	In the event of a sudden downhole increase in pressure, a lower mud pressure would provide a wider drilling window.

Weight on Bit (WOB)	Not immediately increasing WOB if ROP drops through Balder	Drop in ROP through Balder can indicate bit balling, which would only be exacerbated by an increase in WOB.
Fracture characterisation	Acquire LWD image logs through the Balder	Identification of fracture networks within the Balder prone to drilling issues.
Casing points	Avoid setting casing points within the Balder	Interbedded, mechanically weak formations make poor locations for casing points.

402 **Table 2:** List of actions to mitigate against encountering drilling issues through the Balder Formation
403 around the Corona Ridge area.

404

405 Swelling clays and bit balling have been reported through the Balder Formation in a number
406 of the Corona Ridge wells examined (e.g. 213/26-1) despite the use of KCl water-based mud (KCl
407 being an additive meant to inhibit clay swelling). Oil-based muds (OBM) eliminate water from the
408 external phase and therefore would offer greater clay swelling inhibition for future wells drilling
409 through the Balder around the Corona Ridge.

410 In the majority of the wells where drilling issues occur a tricone drill bit was used, with the
411 exception of the Sula/Stelkur well (6104/25-1) in the Faroese sector, where a hybrid bit was used
412 (combination of fixed cutter and roller cone). A key feature of both tricone and hybrid bits is that the
413 nozzles which expel the drilling fluid are located slightly behind and to the side of the drill bit, and are
414 therefore less effective at clearing away a build-up of swelling clays. Therefore, use of a PDC drill bit
415 with central nozzles through the Balder may help retard bit balling, a phenomenon which appears to
416 precede fracture enhancement and drilling fluid loss; see Table 1 where all three uses of PDC bits has
417 not lead to the problems associated with other bits. However, the use of a PDC bit often can lead to
418 a degradation in cuttings quality, and consequently biostratigraphic observations, which has shown to
419 be a critical component in correlating reservoir intervals along the Corona Ridge (Schofield & Jolley
420 2013; Hardman *et al.* 2018).

421 A further drilling consideration for future wells around the Corona Ridge is the placement of
422 casing points. Formations which are interbedded and mechanically weak, such as the Balder Formation

423 around the Corona Ridge, tend to form poor locations to set casing shoes. Future wells around the
424 Corona Ridge therefore may be best cased off before or after the Balder Formation is penetrated.
425 Future studies could also examine the impact a weakened Balder Formation may have on the stability
426 of the overlying Stronsay Group sediments. The North Uist well (213/25-1c) along the Corona Ridge
427 for instance, had major difficulties getting casing through the base of these Stronsay Group sediments,
428 just above a potentially weakened Balder Formation.

429

430 ***Wider Implications for the Petroleum System***

431 The widespread occurrence of drilling fluid losses in wells around the Corona Ridge betrays the
432 presence of permeability within the Balder Formation. The exact nature of this permeability away from
433 the wellbore is unclear, be it within pre-existing fractures, fractures enhanced during drilling or
434 permeable turbidite sediment stringers. However, an increase in background gas within the Balder
435 both in North Uist (213/25-1c) and in Rosebank Main (205/1-1) associated with smaller fractures
436 where no drilling issues occur signifies that the permeability is to an extent natural, and not solely
437 drilling induced. The presence of permeability within the Balder Formation is slightly counter intuitive
438 as it is a laterally extensive formation composed of relatively low permeability claystone, siltstone and
439 volcanic tuffs.

440 It is well established that the Balder Formation forms an effective top seal in other parts of
441 the UK Continental Shelf, notably within the Bressay Discovery in the contiguous North Sea Basin
442 (Underhill 2001). When comparing the Bressay and Rosebank structures side-by-side (Fig. 15), the
443 sands underlying the Balder at Rosebank are water-bearing, despite being within a four-way closure,
444 in contrast to the oil charged sands of Bressay. Fluorescence is, however, reported in ditch cuttings
445 from the Hildasay Member in Rosebank well 213/27-3, suggesting hydrocarbons have migrated through
446 the Hildasay. Notably the Bressay structure has an entirely different genesis to Rosebank and the
447 Corona Ridge. Bressay formed as a result of differential compaction due to an incised fluvial channel
448 (which forms the reservoir) which the Balder Formation drapes (Underhill 2001). Traps formed
449 through differential compaction, or “drape anticlines”, form shortly after reservoir deposition and

450 without tectonic disturbance (Allen & Allen 2005; p. 483). In contrast, inversion anticlines, such as the
451 Rosebank trap (Duncan *et al.* 2009), form due to the reversal of extensional faults during compression
452 (Williams *et al.* 1989). The compressional tectonism associated with the formation of the Rosebank
453 anticline trap therefore may have generated a permeable fracture network which ultimately retarded
454 the sealing capability of the Balder Formation.

455

456 ***Application to other sedimentary basins***

457 This study deconstructs the chain-reaction of events which occur whilst drilling the Balder Formation,
458 which in the study area specifically is prone to swelling. These drilling events all occurred with the use
459 of a water-based drilling mud, which despite the presence of KCl as an inhibitor, still caused the Balder
460 to swell and ball the bit. The swelling within the Balder Formation is linked to the presence of smectitic
461 clays, which are a product of alteration of the original volcanic ash (Knox & Morton 1983; Malm *et al.*
462 1984; Knox & Morton 1988). In addition to volcanic input, smectite-rich sedimentary successions can
463 also be sourced from drainage of large continents (Griffin *et al.* 1968). Within the Gulf of Mexico, for
464 example, swelling smectite clays are termed “gumbo shale” and widely known for drilling issues such
465 as low rates of penetration (Allred & McCaleb 1973; Klein *et al.* 2003; Sameni & Chamkalani 2018).
466 This study’s multidisciplinary approach of placing drilling incidents within the context of regional
467 geological observations, including the tectonic history and environment of deposition, could therefore
468 be applied to other sedimentary basins where similar drilling issues are recorded. We emphasise the
469 need to properly integrate the geological understanding with drilling planning and parameters. This is
470 important in the current exploration drilling backdrop where water-based drilling muds are being
471 increasingly deployed because they are viewed as more environmentally acceptable (Anderson *et al.*
472 2010), and therefore the prospect of swelling clays will continue to be a risk during drilling operations.

473 **Conclusions**

474 A myriad of drilling incidents have been observed whilst drilling the Balder Formation around the
475 Corona Ridge area of the FSB, including bit balling, drilling fluid loss, wellbore ballooning and wellbore
476 collapse, often with multi-million pound cost implications. These drilling phenomena appear linked,

477 effectively forming a drilling chain reaction- bit balling preceding drilling fluid loss, followed by wellbore
478 ballooning. These drilling events can be linked back to the geological history of the basin, in particular
479 to Miocene compression which appears to have inherently weakened the Balder Formation along the
480 Corona Ridge. However, these drilling issues can be mitigated by drill bit selection, particularly through
481 the use of a PDC bit, rather than a tricone (Table 2). Furthermore, the recognition of a permeable
482 Balder Formation around the Corona Ridge has important ramifications for quantifying risk in
483 exploration of the Hildasay sandstone play.

484 Ultimately, this study highlights the importance of integrating regional geological observations,
485 such as tectonic histories, to help fully understand the origin of drilling issues. This multidisciplinary
486 approach, between geology and drilling operations, could be applied to other sedimentary basins
487 globally where drilling issues such as swelling clays and mud losses are reported.

488 **Acknowledgements** This work forms part of the lead author's PhD research, which is funded by a University
489 of Aberdeen College of Physical Sciences Scholarship. This study originally formed part of a talk delivered to the
490 2017 Schlumberger SIS Forum. Well log and drilling data interpretation was performed using Schlumberger
491 Techlog* wellbore software platform. We would like to thank numerous staff at Schlumberger SIS in Aberdeen
492 for useful discussions. DW would also like to thank staff at Chevron's Aberdeen office for important insights on
493 the Rosebank Field, particularly the presence of image logs. Andrew Hurst is thanked for informative discussions
494 regarding smectite clays and their origins. Finally, DW would like to thank members of the VMRC Consortium
495 for helpful feedback on a presentation related to the study, particularly staff at Siccar Point Energy. Two
496 anonymous reviewers are thanked for their detailed reviews which greatly improved the paper.

497

498

499 **References**

500 Ablard, P., Bell, C., Cook, D., Fornasier, I., Poyet, J.-P., Sharma, S., Fielding, K., Lawton, L., Haines, G.,
501 Herkommer, M. A., McCarthy, K., Radakovic, M. & Ulmar, L. 2012. The Expanding role of
502 mudlogging. *Oilfield Review*, **24**, 24-41.

503 Allen, P.A. & Allen, J.R. 2005. Basin Analysis: Principles and Application to Petroleum Play
504 Assessment. Wiley, Chichester.

505 Allred, R. B. & McCaleb, S. B. 1973. Rx for Gumbo Shale Drilling. SPE Drilling and Rocks Mechanics
506 Conference, 22-23 January, Austin, Texas.

507 Anderson, R. L., Ratcliffe, I., Greenwell, H. C., Williams, P. A., Cliffe, S. & Coveney, P. V. 2010. Clay
508 swelling – A challenge in the oilfield. *Earth-Science Reviews*, **98**, 201-216.

509 Archer, S.G., Bergman, S.C., Iliffe, J., Murphy, C.M. & Thornton, M. 2005. Palaeogene igneous rocks
510 reveal new insights into the geodynamic evolution and petroleum potential of the Rockall Trough,
511 NE Atlantic Margin. *Basin Research*, **17**, 171– 201.

* Mark of Schlumberger

- 512 Austin, J.A., Cannon, S.J.C. & Ellis, D. 2014. Hydrocarbon exploration and exploitation West of
513 Shetlands. In: Cannon, S.J.C. & Ellis, D. (eds) *Hydrocarbon Exploration to Exploitation West of Shetlands*.
514 Geological Society, London, Special Publications, **397**, 1–10, <https://doi.org/10.1144/SP397.13>
- 515 Baker Hughes, Kymera Bit Catalogue. 2018.
516 [https://assets.www.bakerhughes.com/system/eb6958df302ce4a7f87b4a35a9692f17_33541_kymera_o](https://assets.www.bakerhughes.com/system/eb6958df302ce4a7f87b4a35a9692f17_33541_kymera_ovr2.pdf)
517 [vr2.pdf](https://assets.www.bakerhughes.com/system/eb6958df302ce4a7f87b4a35a9692f17_33541_kymera_ovr2.pdf). [Accessed 14/10/2018]
- 518 Barton, C. A., Zoback, M. D. & Moos, D. 1995. Fluid flow along potentially active faults in crystalline
519 rocks. *Geology*, **23**, 683-686.
- 520 Bell, J.S. & D.I. Gough. 1979. Northeast-southwest compressive stress in Alberta: Evidence from oil
521 wells. *Earth Planetary Science Letters*, **45**, 475-482.
- 522 Boldreel, L.O. & Andersen, M.S. 1993. Late Paleocene to Miocene compression in the Faeroe–
523 Rockall area. In: Parker, J.R. (ed.) *Petroleum Geology of Northwest Europe: Proceedings of the 4th*
524 *Conference*. Geological Society, London, 1025–1034, <https://doi.org/10.1144/0041025>
- 525 Caenn, R. & Chillingar, G. V. 1996. Drilling fluids: State of the art. *Journal of Petroleum Science and*
526 *Engineering*, **14**, 221-230.
- 527 Cheatham, C.A. & Nahm, J.J. 1990. Bit balling in water-reactive shale during full-scale drilling rate
528 tests. In: IADC/SPE Drilling Conference. SPE, Houston. Paper 19926.
- 529 Cook, J., Growcock, F., Guo, Q., Hodder, M. & van Oort, E. 2011. Stabilizing the wellbore to
530 prevent lost circulation. *Oilfield Review*, **23**, 4-13.
- 531 Dart, R. L. & Zoback, M. L. 1989. Wellbore breakout stress analysis within the central and eastern
532 continental United States. *The Log Analyst*, **30**, 12-25.
- 533 Doré, A.G., Lundin, E.R., Kusznir, N.J. & Pascal, C. 2008. Potential mechanisms for the genesis of
534 Cenozoic domal structures on the NE Atlantic margin: pros, cons and some new ideas. In: Johnson,
535 H., Doré, A.G., Gatliff, R.W., Holdsworth, R.W., Lundin, E. & Ritchie, J.D. (eds) *The Nature of*
536 *Compression in Passive Margins*. Geological Society, London, Special Publications, **306**, 1–26,
537 <https://doi.org/10.1144/SP306.1>
- 538 Duncan, L., Helland-Hansen, D. & Dennehy, C. 2009. The Rosebank Discovery, A new play type in
539 intra basalt reservoirs of the North Atlantic volcanic province. In: 6th European Production and
540 Development Conference and Exhibition (DEVEX), Abstracts. Chevron Upstream Europe,
541 Aberdeen, http://www.devex-conference.org/pdf/Presentations_2009/2A1605%20Chevron%20The%20Rosebank%20Discovery%20-%20new%20play%20type%20in%20intra%20basalt%20reservoirs%20of%20the%20North%20Atlantic%20volcanic%20province.pdf
- 542
543
- 544 Ellis, D., Jolley, D.W., Passey, S.R. & Bell, B.R. 2009. Transfer zones: The application of new
545 geological information from the Faroe Islands applied to the offshore exploration of intra basalt and
546 sub-basalt strata. In: Varming, T. & Ziska, H. (eds) *Faroe Islands Exploration Conference: Proceedings of*
547 *the 2nd Conference*. Annals Societatis Scientiarum Faerensis, Supplementum, **50**, 205–226.
548
- 549 Ellis, D. & Stoker, M. S. 2014. The Faroe-Shetland Basin: a regional perspective from the Paleocene
550 to the present day and its relationship to the opening of the North Atlantic Ocean. In: Cannon, S.J.C.
551 & Ellis, D. (eds) *Hydrocarbon Exploration to Exploitation West of Shetlands*. Geological Society, London,
552 Special Publications, **397**, 11-31, <https://doi.org/10.1144/SP397.1>

- 553 German, V., Pak, M. & Azarm, M. 2015. Conical Diamond Element Bit Sets New Performance
554 Benchmarks Drilling Extremely Hard Carbonate/Chert Formations, Perm Region Russia. SPE/IADC
555 Drilling Conference and Exhibition, London, 17-19 March.
- 556 Griffin, J. J., Windom, H. & Goldberg, E. D. 1968. *Deep-Sea Research*, **15**, 433-459.
- 557 Grindhaug, G., 2012. Statoil hard rock drilling experience. *In: Norwegian Drilling Technologies Expo.*
558 IEA Geothermal, Oslo.
- 559 Hardman, J. P. A., Schofield, N., Jolley, D. W., Holford, S. P., Hartley, A. J., Morse, S., Underhill, J. R.,
560 Watson, D. A. & Zimmer, E. H. 2018a. Prolonged dynamic support from the Icelandic plume of the
561 NE Atlantic Margin. *Journal of the Geological Society, London*. **175**, 396-410,
562 <https://doi.org/10.1144/jgs2017-088>
- 563 Hardman, J., Schofield, N., Jolley, D., Hartley, A., Holford, S. & Watson, D. 2018b. Controls on the
564 distribution of volcanism and intra-basaltic sediments in the Cambo-Rosebank region, West of
565 Shetland. *Petroleum Geoscience*, **xx**, xxx-xxx, <https://doi.org/10.1144/petgeo2017-061>
- 566 Hariharan, P.R. & Azar, J.J. 1996. PDC bit hydraulics design, profile are key to reducing balling. *Oil &*
567 *Gas Journal*. **94** (50), 58e63.
- 568 Helland-Hansen, D. 2009. Rosebank – challenges to development from a subsurface perspective. *In:*
569 Varming, T. & Ziska, H. (eds) *Faroe Islands Exploration Conference: Proceedings of the 2nd Conference.*
570 *Annales Societatis Scientiarum Faroensis, Supplementum*, **50**, 241–245.
- 571 Helstrup, O. A., Chen, Z. & Rahman, S. S. 2004. Time Dependent wellbore instability in naturally and
572 fractured formations. *Journal of Science and Engineering*, **43**, 113-128.
- 573 Hillis, R. R. & Williams, A. F. 1992. Borehole breakouts and stress analysis in the Timor Sea. *In:*
574 Hurst, A., Griffiths, C. M. & Worthington, P. F. (eds) *Geological Applications of Wireline Logs II.*
575 Geological Society, London, Special Publications, **65**, 157-168.
- 576 Holford, S. P., Green, P. F., Duddy, I. R., Turner, J. P., Hillis, R. R. & Stoker, M. S. 2009. Regional
577 intraplate exhumation episodes related to plate-boundary deformation. *GSA Bulletin*, **121**, 1611-1628.
- 578 Holford, S. P., Tassone, D. R., Stoker, M. S. & Hillis, R. R. 2016. Contemporary stress orientations in
579 the Faroe-Shetland region. *Journal of the Geological Society, London*. **173**, 142-152, doi:10.1144/jgs2015-
580 048
- 581 IHS Markit, 2018. <https://www.ihsmarkit.com/products/oil-gas-drilling-rigs-offshore-day-rates.html>.
582 [Accessed 03/04/2018]
583
- 584 Jepson, G., King, R. C., Holford, S., Bailey, A. H. E. & Hand, M. in press. In-situ stress and natural
585 fractures in the Carnarvon Basin, Northwest Shelf, Australia. *Exploration Geophysics*
586
- 587 Klein, A. L., Aldea, C., Bruton, J. R. & Dobbs, W. R. 2003. Field Verification: Invert Mud Performance
588 from Water-Based Mud in Gulf of Mexico Shelf. SPE Annual Technical Conference and Exhibition, 5-
589 8 October, Denver, Colorado.
590
- 591 Knox, R.W.O'B. & Morton, A.C. 1983. Stratigraphical distribution of Early Palaeogene pyroclastic
592 deposits in the North Sea Basin. *Proceedings of the Yorkshire Geological Society*, **44**, 355–363,
593 <https://doi.org/10.1144/pygs.44.3.355>
594
- 595 Knox, R.W.O'B. & Holloway, S. 1992. Lithostratigraphical nomenclature of the UK North Sea. I.
596 Paleogene of the Central and Northern North Sea. *In: Knox, R.W.O'B. & Cordey, W.G. (eds)*
597 *Lithostratigraphic Nomenclature of the UK North Sea*. British Geological Survey, Keyworth, 63–72.

- 598 Knox, R.W.O'B. & Morton, A.C. 1988. The record of early Tertiary N Atlantic volcanism in
599 sediments of the North Sea Basin. *In: Morton, A.C. & Parson, L. M. (eds) Early Tertiary Volcanism and*
600 *the Opening of the NE Atlantic*. Geological Society, London, Special Publications, **39**, 407–419,
601 <https://doi.org/10.1144/GSL.SP.1988.039.01.36>
- 602 Lamers, E. & Carmichael, S.M.M. 1999. The Paleocene deepwater sandstone play west of Shetland.
603 *In: Fleet, A.J. & Boldy, S.A.R. (eds) Petroleum Geology of Northwest Europe: Proceedings of the 5th*
604 *Conference*. Geological Society, London, 645–659, <https://doi.org/10.1144/0050645>
- 605 Malm, A.O., Christensen, O.B., Furnes, H., Løvlie, R., Rueslåtten, H. & Østby, K.L. 1984. The Lower
606 Tertiary Balder Formation: an organogenic and tuffaceous deposit in the North Sea region. *In:*
607 *Spencer, A.M. (ed.) Petroleum Geology of the North European Margin*. Graham and Trotman, London.
608
- 609 Mark, N. J., Schofield, N., Pugliese, S., Watson, D., Holford, S., Muirhead, D., Brown, R. & Healy, D.
610 2018. Igneous intrusions in the Faroe Shetland basin and their implications for hydrocarbon
611 exploration; new insights from well and seismic data. *Marine and Petroleum Geology*, **92**, 733-753.
- 612 McLean, M. R. & Addis, M. A. 1990. Wellbore Stability: the Effect of Strength
613 Criteria on Mud Weight Recommendations. SPE Annual Technical Conference and
614 Exhibition, 23-26 September, New Orleans, Louisiana,
615 <https://doi.org/10.2118/20405-MS>
616
- 617 Millet, J. M., Hole, M. J. & Jolley, D. W. 2014 A fresh approach to ditch cuttings analysis as an aid to
618 exploration in areas affected by large igneous province (LIP) volcanism. *In: Cannon, S.J.C. & Ellis, D.*
619 *(eds) Hydrocarbon Exploration to Exploitation West of Shetlands*. Geological Society, London, Special
620 Publications, **397**, 193-207, <https://doi.org/10.1144/SP397.2>
- 621 Millett, J. M., Hole, M.J., Jolley, D.W., Schofield, N. & Campbell, E. 2015. Frontier exploration and the
622 North Atlantic Igneous Province: new insights from a 2.6 km offshore volcanic sequence in the NE
623 Faroe–Shetland Basin. *Journal of the Geological Society, London*, **173**, 320–336, [https://doi.org/10.](https://doi.org/10.1144/jgs2015-069)
624 [1144/jgs2015-069](https://doi.org/10.1144/jgs2015-069)
- 625 Millett, J.M., Wilkins, A.D., Campbell, E., Hole, M. J., Taylor, R. A., Healy, D., Jerram, D., Jolley, D.
626 W., Planke, S., Archer, S. G. & Blischke, A.. 2016. The geology of offshore drilling through basalt
627 sequences: Understanding operational complications to improve efficiency. *Marine and Petroleum*
628 *Geology*, **77**, 1177–1192.
- 629 Mizusaki, A. M. P., Petrini, R., Bellieni, P., Comin-Chiaramonti, P., Dias, J., De Min, A. & Piccirillo, E.
630 M. Basalt Magmatism along the passive continental margin of SE Brazil (Campos basin). *Contributions*
631 *to Mineralogy and Petrology*.
- 632 Mudge, D.C. 2014. Regional controls on Lower Tertiary sandstone distribution in the North Sea and
633 NE Atlantic margin basins. *In: McKie, T., Rose, P.T.S., Hartley, A.J., Jones, D.W. & Armstrong, T.L.*
634 *(eds) Tertiary Deep-Marine Reservoirs of the North Sea Region*. Geological Society, London, Special
635 Publications, **403**, 17–42, <https://doi.org/10.1144/SP403.5>
- 636 Norrish, K. 1954. The swelling of montmorillonites. *Discussions of the Faraday Society*, **18**, 120-134.
- 637 O'Brien, D. E & Chenevert, M. E. 1973. Stabilizing Sensitive Shales with Inhibited, Potassium-Based
638 Drilling Fluids. *Journal of Petroleum Technology*, **25**, 1089-1100.
- 639 Osborne, M. J. & Swarbrick, R. E. 1997. Mechanisms for generating overpressure in sedimentary
640 basins: a reevaluation. *AAPG Bulletin*, **81**, 1023-1041.

- 641 Plumb, R. A. & Hickman, S. H. 1985. Stress-induced borehole elongation: A comparison between the
642 four-arm dipmeter and the borehole televiwer in the Auburn Geothermal Well. *Journal of*
643 *Geophysical Research*, **90**, 5513-5521.
- 644 Poppitt, S., Duncan, L.J., Preu, B., Fazzari, F. & Archer, J. 2016. The influence of volcanic rocks on the
645 characterization of Rosebank Field—new insights from ocean-bottom seismic data and geological
646 analogues integrated through interpretation and modelling. In: Bowman, M. & Levell, B. (eds)
647 *Petroleum Geology of NW Europe: 50 Years of Learning – Proceedings of the 8th Petroleum Geology*
648 *Conference*. Geological Society, London. First published online December 15, 2016,
649 <https://doi.org/10.1144/PGC8.6>
- 650 Rickard, W., Bailey, A., Pahler, M., Cory, S., 2014. Kymera™ hybrid bit technology reduces drilling
651 cost. In: *Thirty-ninth Workshop on Geothermal Reservoir Engineering*. Stanford, California, 1-12.
- 652 Rider, M. & Kennedy, M. 2011. *The Geological Interpretation of Well Logs*, 3rd edn. Rider-French,
653 Glasgow.
- 654 Ritchie, J.D., Johnson, H.D., Quinn, M.F. & Gatliff, R.W. 2008. Cenozoic compressional deformation
655 within the Faroe–Shetland Basin and adjacent areas. In: Johnson, H.D., Doré, A.G., Holdsworth, R.E.,
656 Gatliff, R.W., Lundin, E.R. & Ritchie, J.D. (eds) *The Nature and Origin of Compression in Passive*
657 *Margins*. Geological Society, London, Special Publications, 306, 121–136,
658 <https://doi.org/10.1144/SP306.5>
- 659 Ritchie, J.D., Ziska, H., Johnson, H. & Evans, D. (eds) 2011. *Geology of the Faroe–Shetland Basin and*
660 *Adjacent Areas*. British Geological Survey Research Report, RR/11/01; Jarðfeingi Research Report,
661 RR/11/01.
- 662 Sameni, A. & Chamkalani, A. 2018. Application of Least Square Support Vector Machine as a
663 Mathematical Algorithm for Diagnosing Drilling Effectively in Shaly Formations. *Journal of Petroleum &*
664 *Science Technology*, **8**, 3-16.
- 665 Schlumberger, Smith Bits catalogue. 2018.
666 https://www.slb.com/~media/Files/smith/catalogs/bits_catalog.pdf [Accessed 27 May 2018].
- 667 Schofield, N. & Jolley, D. W. 2013. Development of intra-basaltic lava-field drainage systems within
668 the Faroe-Shetland Basin. *Petroleum Geoscience*, **19**, 273-288.
- 669 Schofield, N., Jolley, D., Holford, S., Archer, S., Watson, D., Hartley, A., Howell, J., Muirhead, D.,
670 Underhill, J. & Green, P. 2017. Challenges of future exploration within the UK Rockall Basin. In:
671 Bowman, M. & Levell, B. (eds) *Petroleum Geology of NW Europe: 50 Years of Learning – Proceedings of*
672 *the 8th Petroleum Geology Conference*. First published online February 16, 2017, [https://doi.org/](https://doi.org/10.1144/PGC8.37)
673 [10.1144/PGC8.37](https://doi.org/10.1144/PGC8.37)
- 674 Scotchman, I. C., Carr, A. D. & Parnell, J. Hydrocarbon generation modelling in a multiple rifted and
675 volcanic basin: a case study in the Foinaven Sub-basin, Faroe-Shetland Basin, UK Atlantic Margin.
676 *Scottish Journal of Geology*, **42**, 1-19.
- 677 Scotchman I.C., Doré A.G. & Spencer A.M. 2016. Petroleum systems and results of exploration on
678 the Atlantic margins of the UK, Faroes & Ireland: what have we
679 learnt? In: Bowman M. & Levell B. (eds) *Petroleum Geology of NW Europe: 50 Years of Learning –*
680 *Proceedings of the 8th Petroleum Geology Conference*. Geological Society, London, first published online
681 October 27, 2016, <https://doi.org/10.1144/PGC8.14>
- 682 Siccar Point Energy. 2018. <http://www.siccarpointenergy.co.uk/our-portfolio/northern-gas-are>
683 [Accessed 03/04/2018]

- 684 Stoker, M. & Varming, T. 2011. Cenozoic (sedimentary). In: Ritchie, J., Ziska, H., Johnson, H. & Evans,
685 D. (eds) *Geology of the Faroe–Shetland Basin and Adjacent Areas*. British Geological Survey
686 Research Report, RR/11/01, Jarðfeingi Research Report, RR/11/01, 151–208.
- 687 Swarbrick, R. E., and Osborne, M. J. 1998. Mechanisms that generate abnormal pressures: An
688 overview. In: Law, B. E., Ulmishek, G. F. & Slavin, V. I. (eds) *Abnormal pressures in hydrocarbon*
689 *environments*. AAPG Memoir, **70**, 13–34.
- 690 Underhill, J. R. 2001. Controls on the genesis and prospectivity of Paleogene palaeogeomorphic
691 traps, East Shetland Platform, UK North Sea. *Marine and Petroleum Geology*, **18**, 259–281.
- 692 Ward, C. & Clark, R. 1998. Anatomy of a ballooning borehole using PWD. Overpressures in
693 Petroleum Exploration Workshop, Pau, France, 7-8 April.
- 694 Warren, T. M. Penetration-Rate Performance of Roller-Cone Bits. *SPE Drilling Engineering*, March, 9-
695 18.
- 696 Watson, D., Schofield, N. et al. 2017. Stratigraphic overview of Palaeogene tuffs in the Faroe–
697 Shetland Basin, NE Atlantic Margin. *Journal of the Geological Society, London*, **174**, 627–645,
698 <https://doi.org/10.1144/jgs2016-132>
- 699 Wensaas, L., Aagaard, P., Berre, T. & Roaldset, E. 1998. Mechanical properties of North Sea Tertiary
700 mudrocks: investigations by triaxial testing of side-wall cores. *Clay Minerals*, **33**, 171–183.
- 701 Williams, G. D., Powell, C. M. & Cooper, M. A. 1989. Geometry and kinematics of inversion
702 tectonics. In: Cooper, M. A. & Williams, G. D. (eds) *Inversion Tectonics*. Geological Society, London,
703 Special Publication, **44**, 3–15.
- 704 White, R. & McKenzie, D. 1989. Magmatism at rift zones: the generation of volcanic continental
705 margins and flood basalts. *Journal of Geophysical Research*, **94**, 7685–7729.
- 706 York, P., Pritchard, D., Dodson, J. K., Dodson, J. K., Rosenberg, S., Gala, D. & Utama, B. 2009.
707 Eliminating Non-Productive Time Associated with Drilling Troubled Zones. In: *Offshore Technology*
708 *Conference*, Houston. Paper 20220.
- 709 Zoback, M. D. 2010. *Reservoir Geomechanics*. Cambridge University Press.
- 710 Zoback, M., Barton, C., Brudy, M., Castillo, D., Finkbeiner, T., Grollmund, B., Moos, D., Peska, P.,
711 Ward, C. & Wiprut, D., 2003, Determination of Stress Orientation and Magnitude in Deep
712 Wells. *International Journal of Rock Mechanics and Mining Sciences*, **40**, 1049–76.

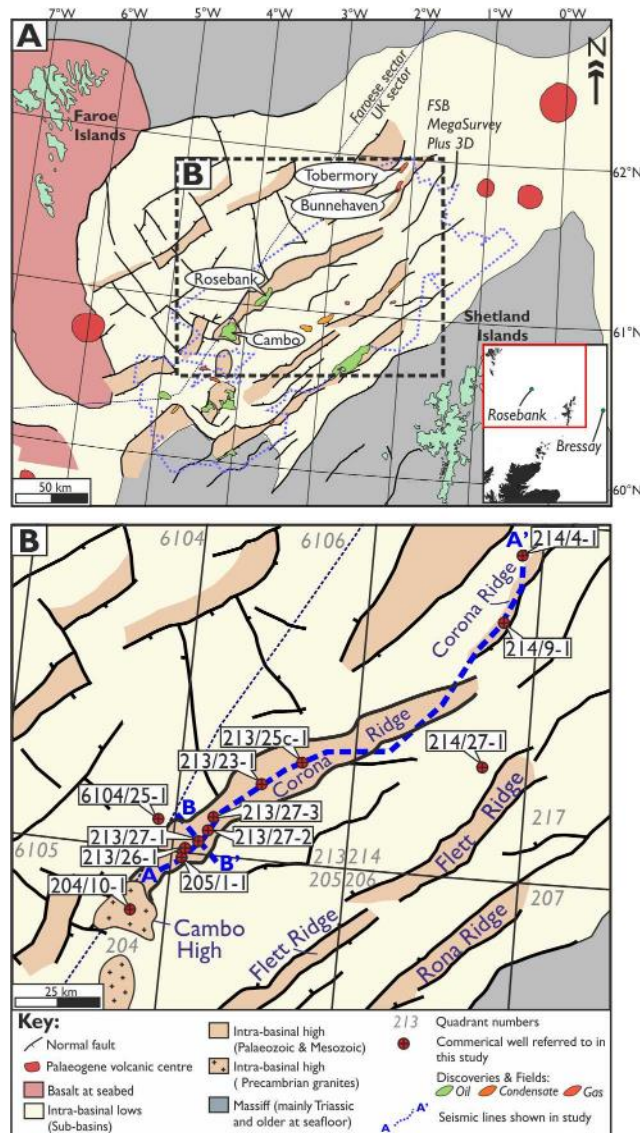
713

714

715 **Figure Captions**

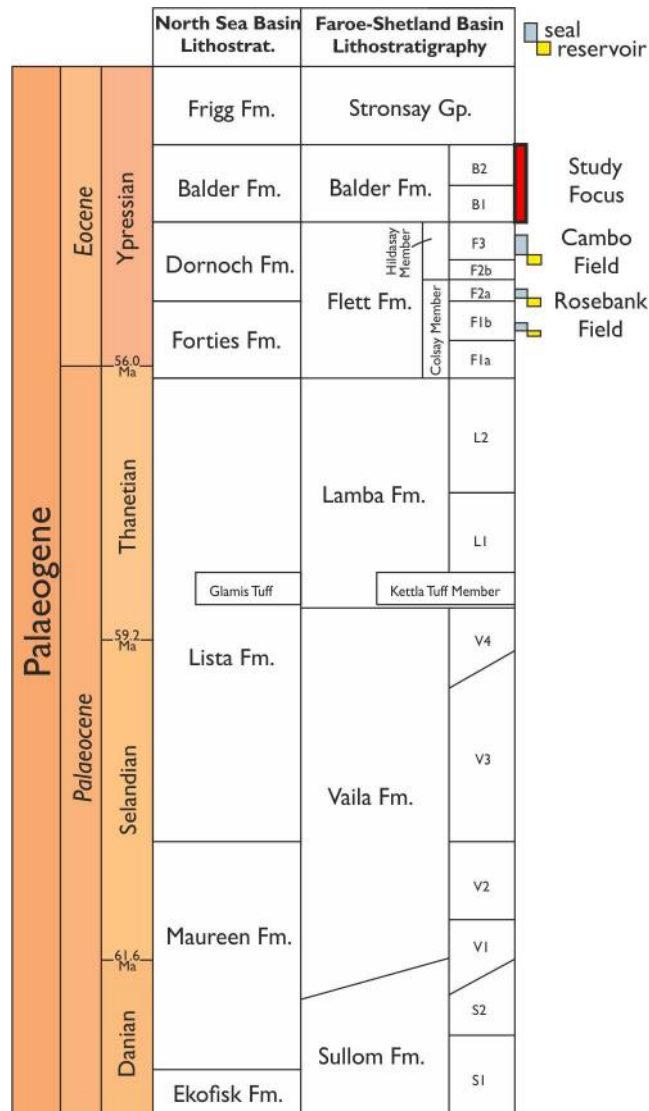
716

717



718
 719
 720
 721
 722
 723
 724
 725
 726
 727

Fig. 1. (A) Map of the Farøe-Shetland Basin with main tectonic elements. **(B)** More localised map, showing the location of this study's focus, including the wells and seismic lines described in this paper. Base map adapted from Ellis *et al.* (2009), and Corona Ridge elements modified based on Hardman *et al.* 2018b.

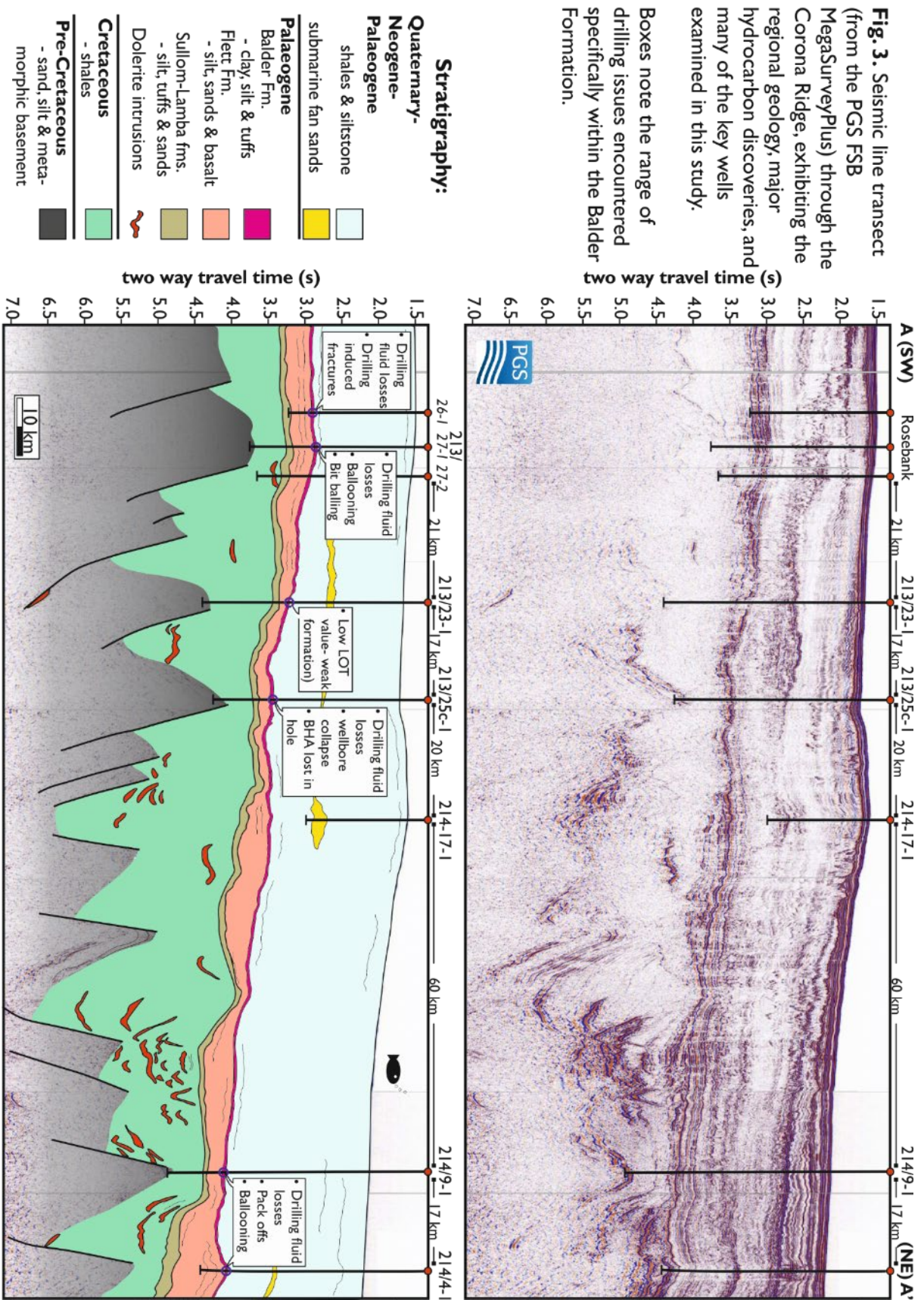


728

729 **Fig. 2.** Lithostratigraphy of the Palaeocene to lower Eocene in the FSB, and their lateral equivalents
 730 in the North Sea. Chart adapted from Ritchie *et al.* (2011), with revision of Colsay and Hildasay
 731 members of the Flett Fm. from Schofield *et al.* 2017.

732

Fig. 3. Seismic line transect (from the PGS FSB MegaSurveyPlus) through the Corona Ridge, exhibiting the regional geology, major hydrocarbon discoveries, and many of the key wells examined in this study. Boxes note the range of drilling issues encountered specifically within the Balder Formation.



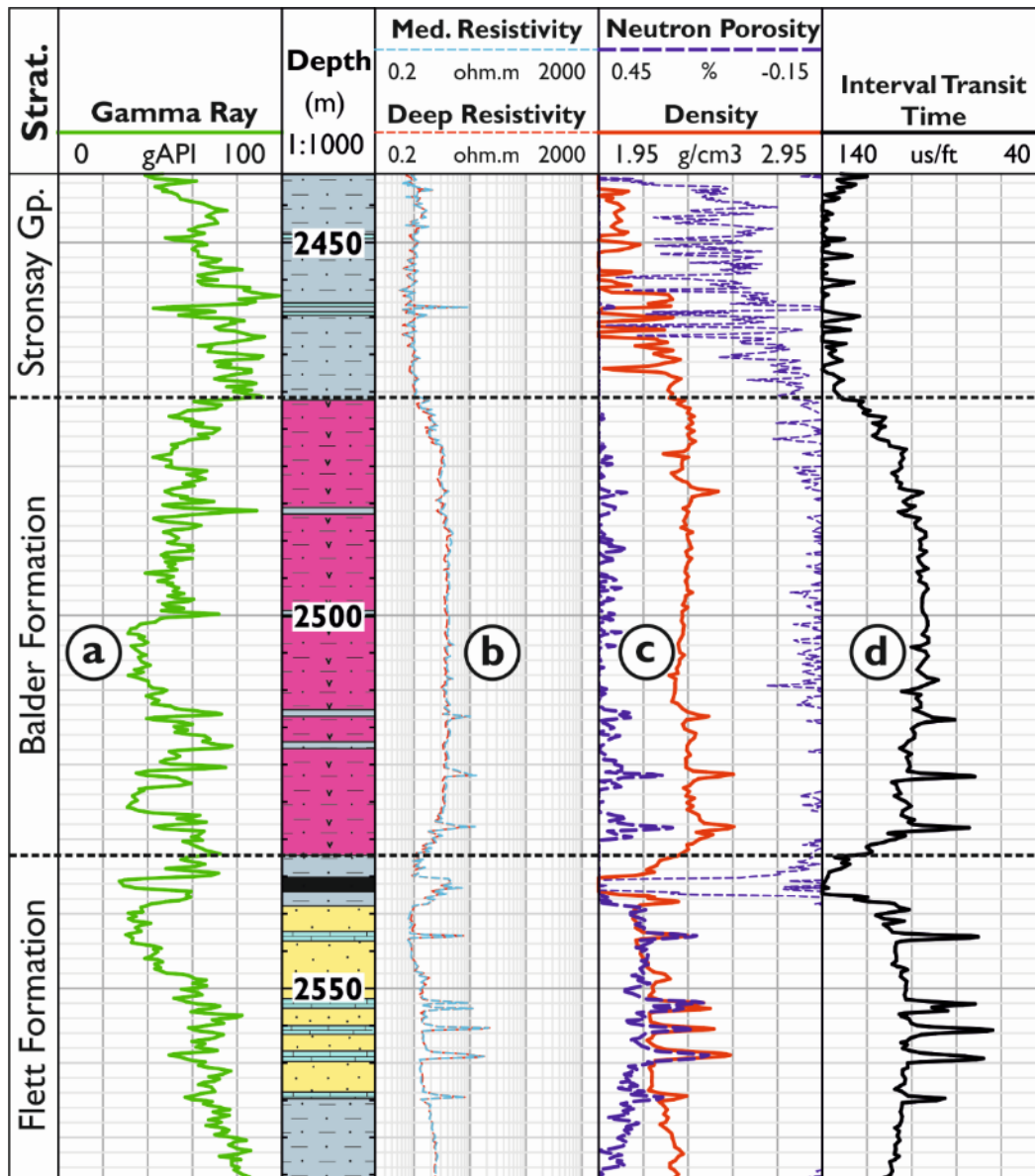
733

734

735

Fig. 3. Seismic line transect (from the PGS FSB MegaSurveyPlus) through the Corona Ridge, exhibiting the regional geology, major hydrocarbon discoveries, and many of the key wells examine

736 in this study. Boxes note the range of drilling issues encountered specifically within the Balder
 737 Formation.
 738

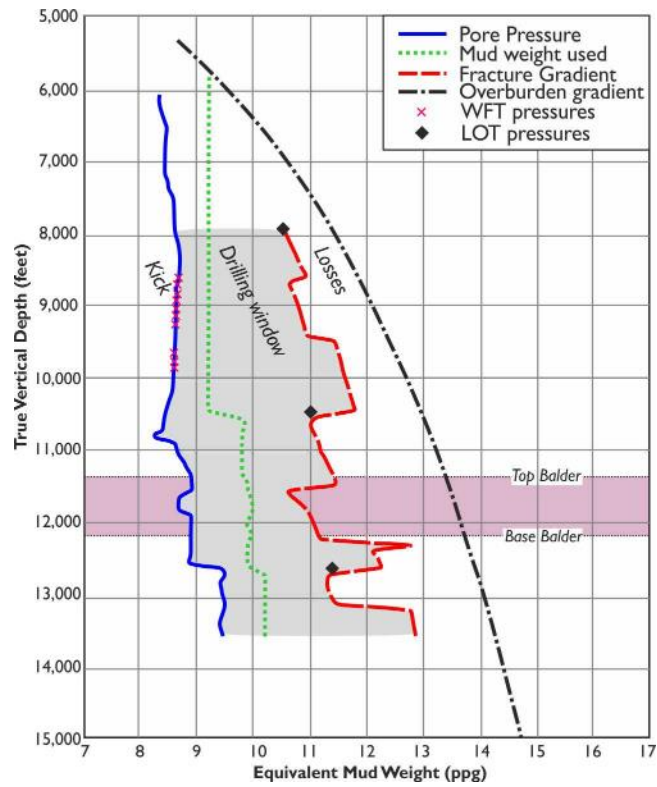


739 Sandstone Claystone/Siltstone coal Limestone Tuffaceous claystone

740

741 **Fig. 4.** Typical well log character of the Balder Formation in the FSB, from well 6104/25-1, manifested
 742 in a low, serrated gamma profile (a), resistivity slightly higher than shale (b), a density/neutron
 743 separation typical of shale (c) and a bell-shaped interval-transit time profile (d).

744



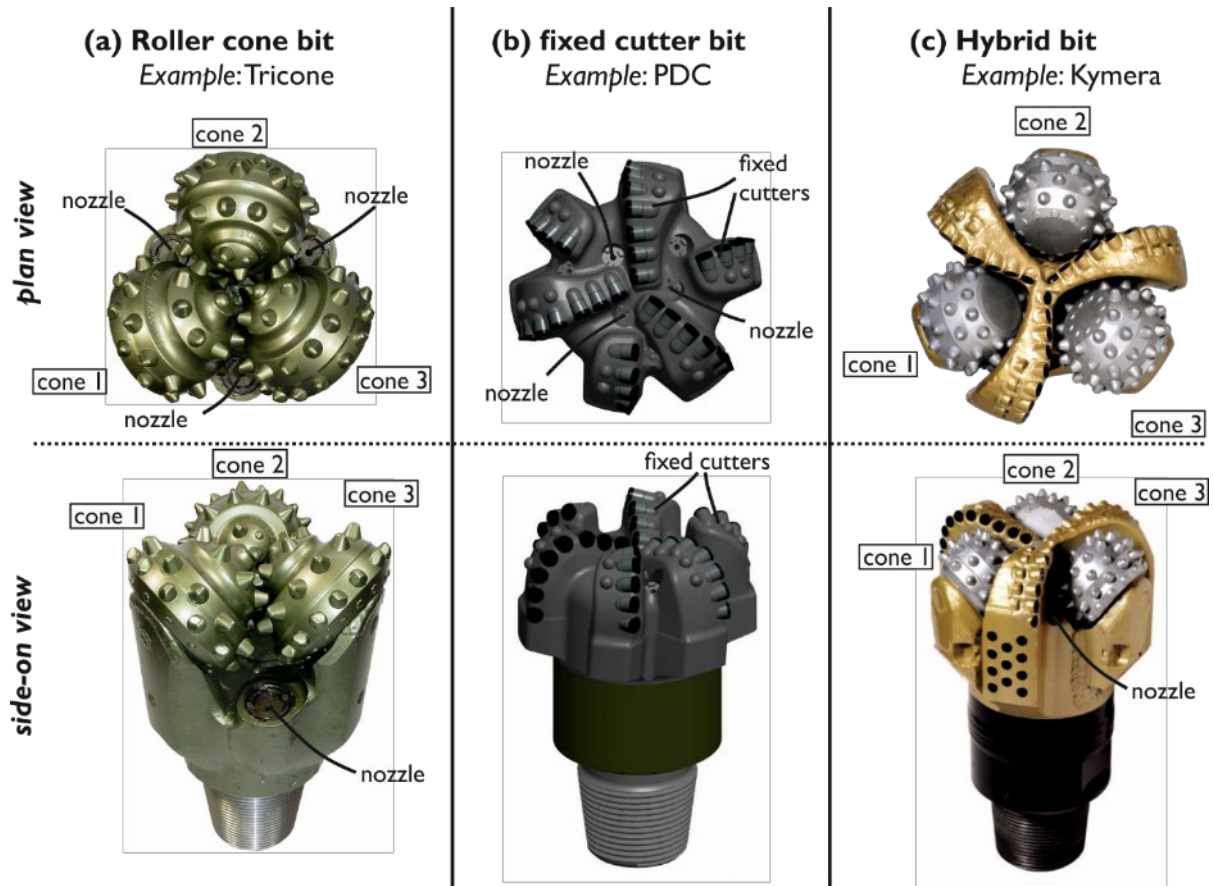
745

746

747 **Fig. 5.** An example of a drilling window plot, from Tobermory (well 214/4-1) End of Well Report. In
 748 this example, as well as all other wells examined, the mud weight (pounds per gallon [ppg]) does not
 749 appear to be set higher than the fracture gradient of the Balder Formation, yet drilling fluid losses still
 750 occurred.

751

752

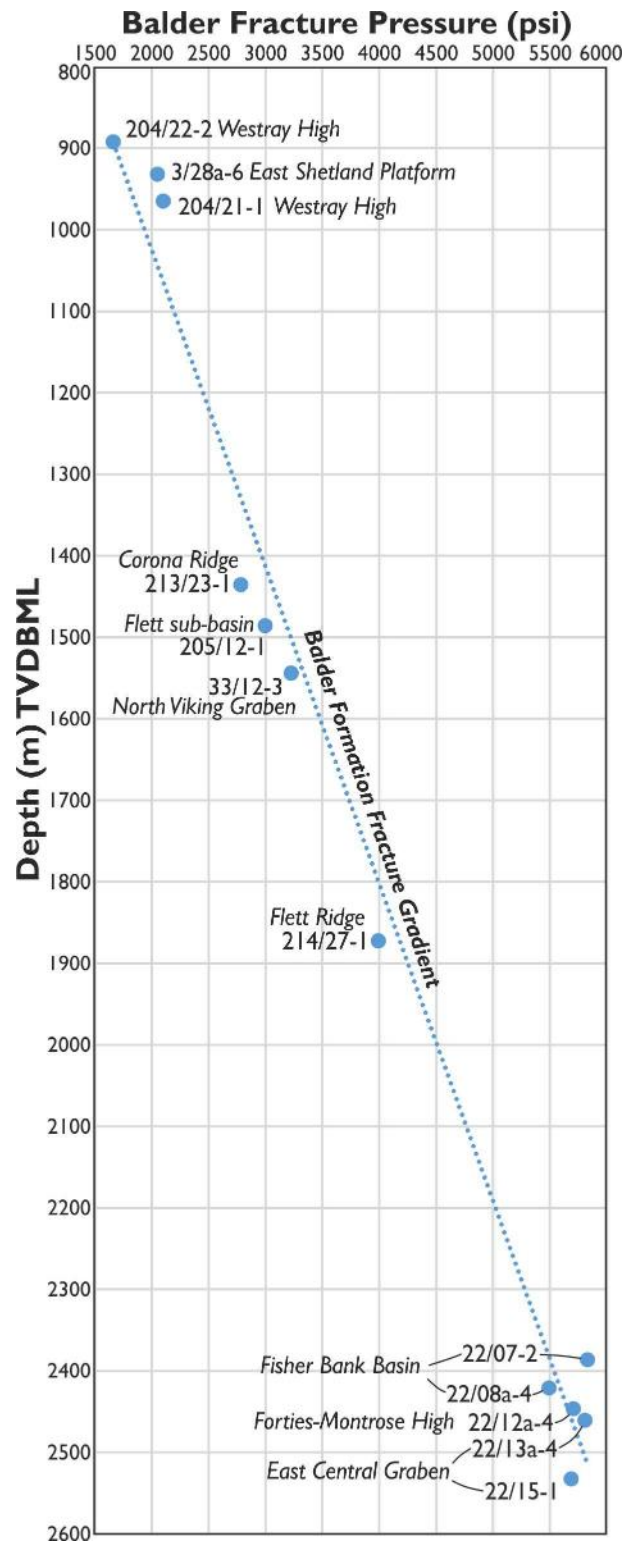


753

754

755 **Fig. 6.** Different types of drill bit commonly used to drill through the Balder Formation around the
 756 Corona Ridge. The nozzles in (a) tricone and (c) Kymera bits are located to the side and further back
 757 from the front of the bit, compared to a (b) PDC bit. Tricone and PDC bits from Schlumberger drilling
 758 catalogue (2018), and hybrid bit from Baker Hughes catalogue (2018).

759



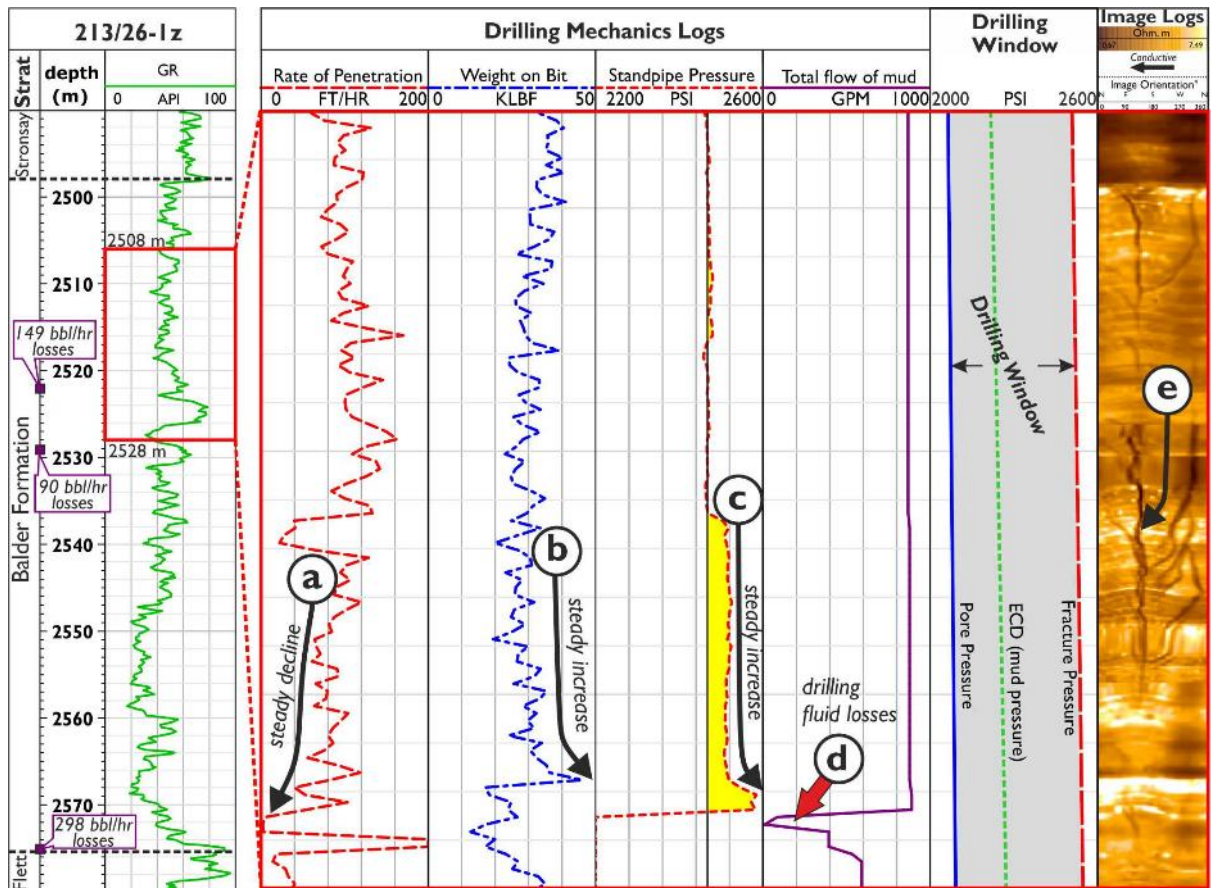
760

761 **Fig. 7.** Regional fracture pressure gradient for the Balder Formation around the Corona Ridge. The
 762 LOT data is from the Balder Formation from wells in the FSB and North Sea.

763

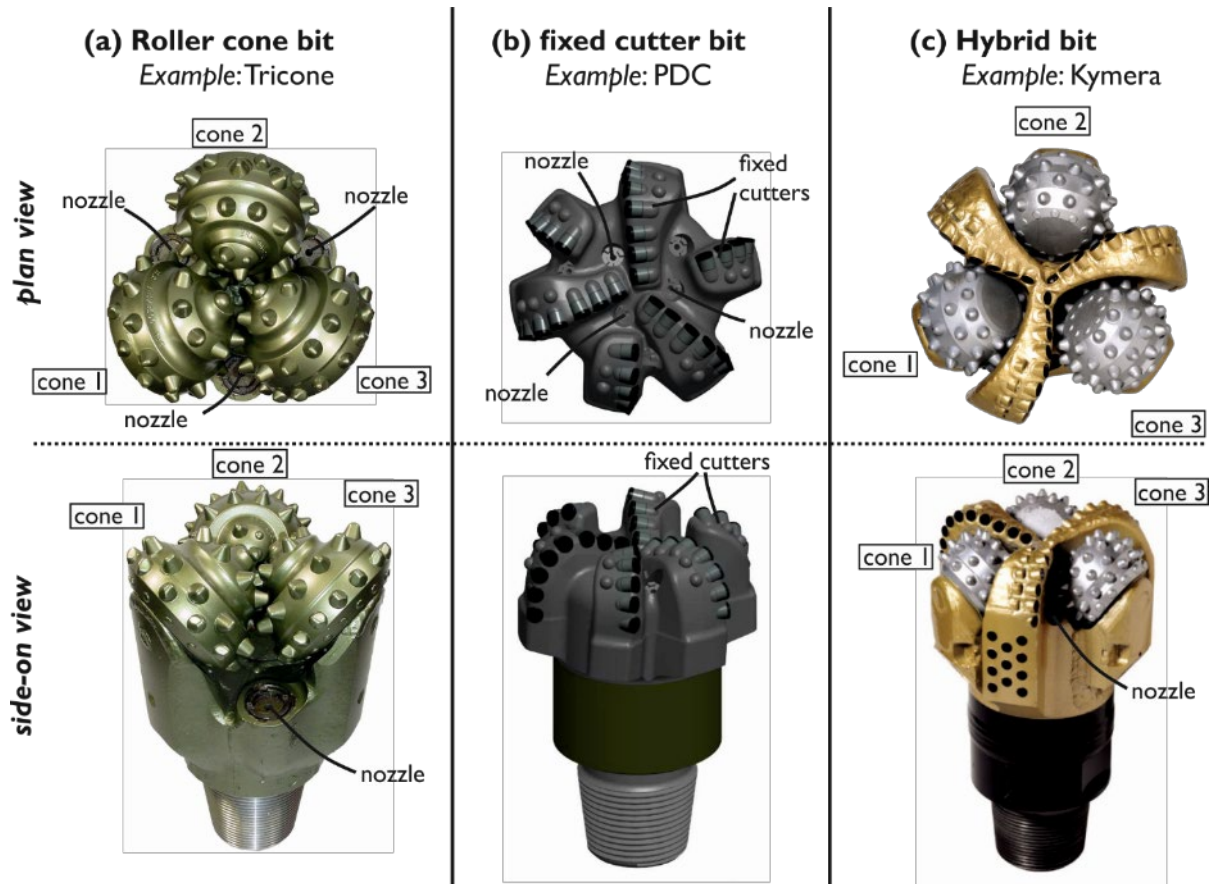
764

765



766
 767 **Fig. 8.** Drilling properties through the Balder Formation in well 213/26-1z. A notable reduction in the
 768 rate of penetration is observed (a), despite the fact the weight on the bit (b) is increased. The increase
 769 in standpipe pressure (c) in therefore indicative of bit balling. Drilling fluid loss (d) is initiated shortly
 770 after the recognition of bit balling. The fluid losses are associated with a conductive fracture network
 771 (e), recognised in image logs. Three separate zones of drilling fluid loss occur (highlighted on the depth
 772 track on the left).

773



774



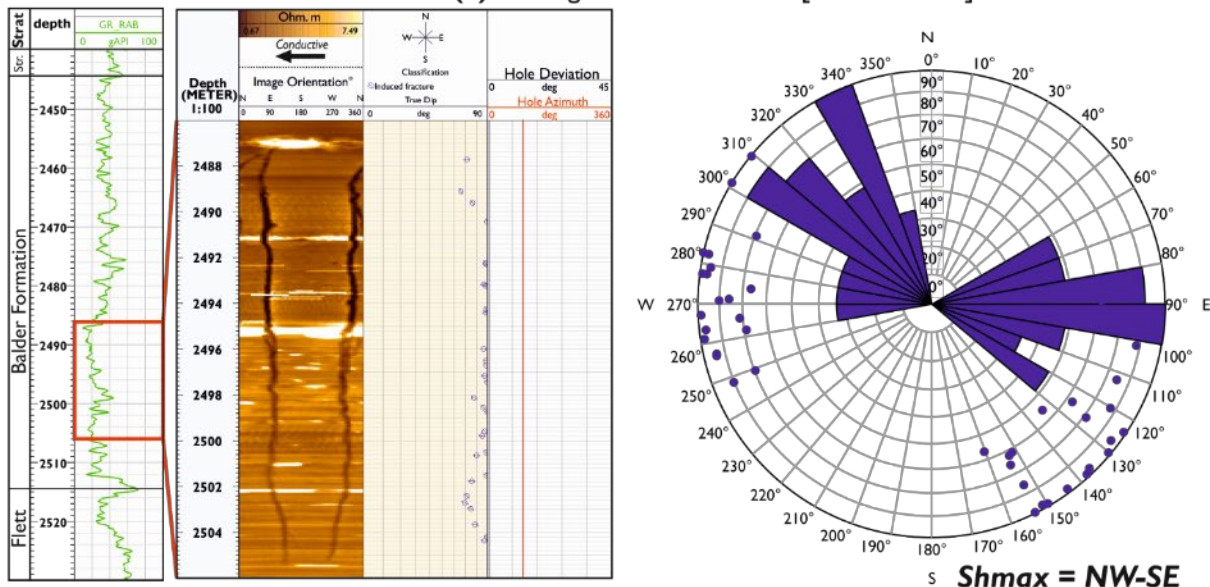
775

776

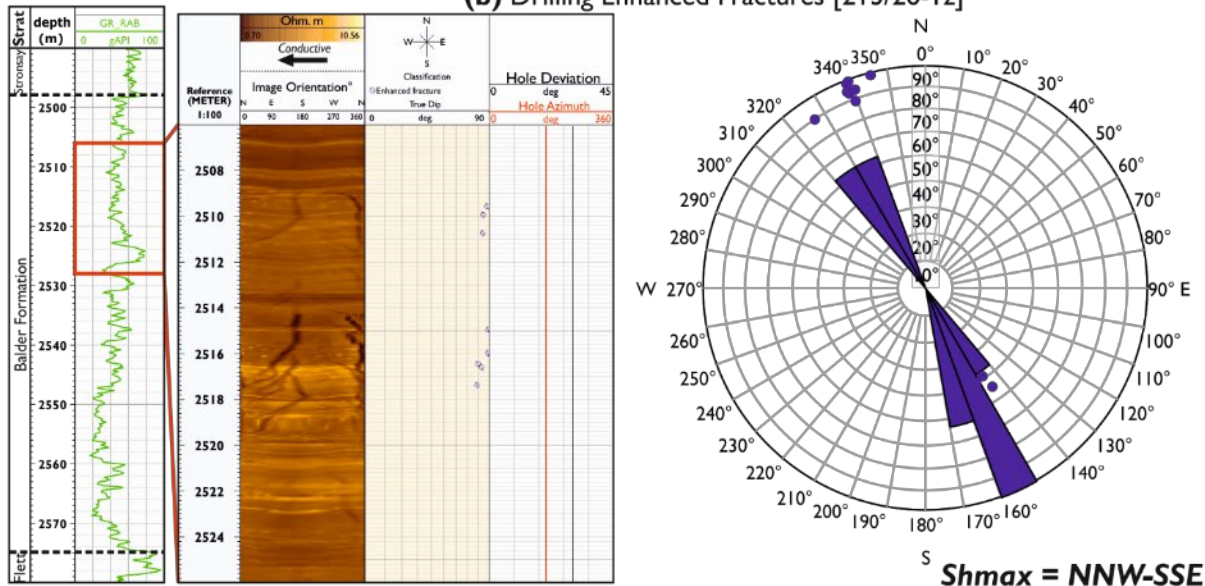
777 **Fig. 9.** Examples of bit balling of a tricone drill bit. Images courtesy of John Jong & Jon Royds, JX
 778 Nippon Oil & Gas Exploration.

779

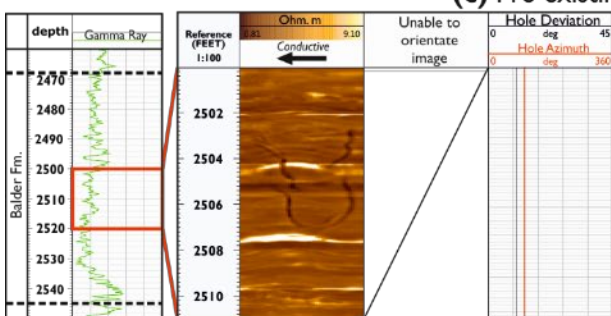
(a) Drilling Induced Fractures [well 213/26-1]



(b) Drilling Enhanced Fractures [213/26-1z]



(c) Pre-existing/natural fractures [205/1-1]

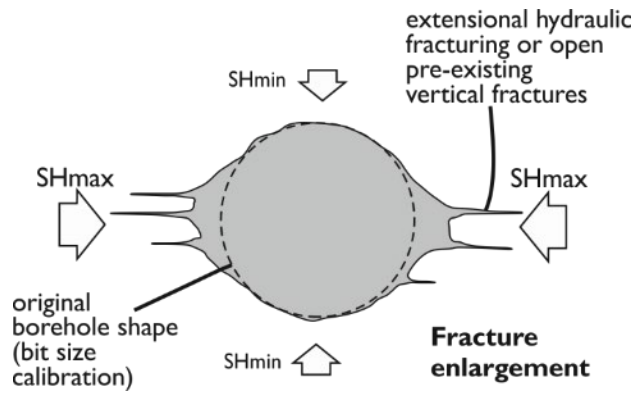


780

781

782 **Fig. 10.** The drilling induced fractures within 213/26-1 (A) are orientated NW-SE, implying a
783 maximum compressive stress (σ_{Hmax}) in the same direction. Drilling enhanced fractures within
784 213/26-1z (B) are orientated NNW-SSE. There are also natural fractures (C) within the Balder in
785 205/1-1; note this image log was not able to be orientated.

786

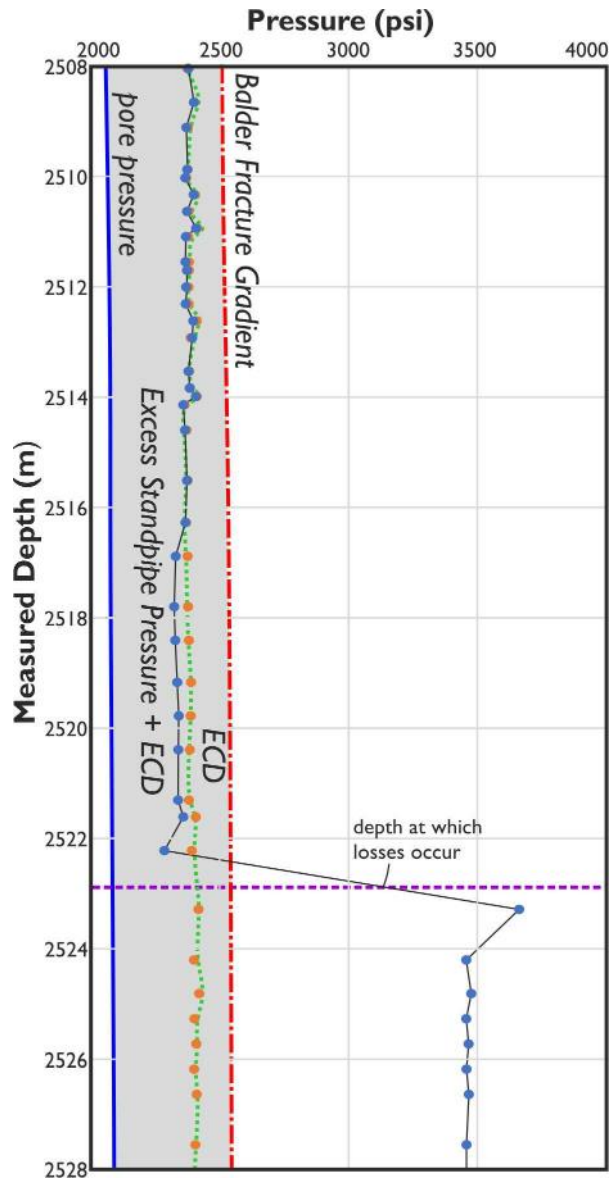


787

788

789 **Fig. 11.** Fracture enlargement (i.e. drilling induced and enhanced fractures) form parallel with the
 790 maximum horizontal stress (SH_{max}). From Hillis & Williams (1992).

791

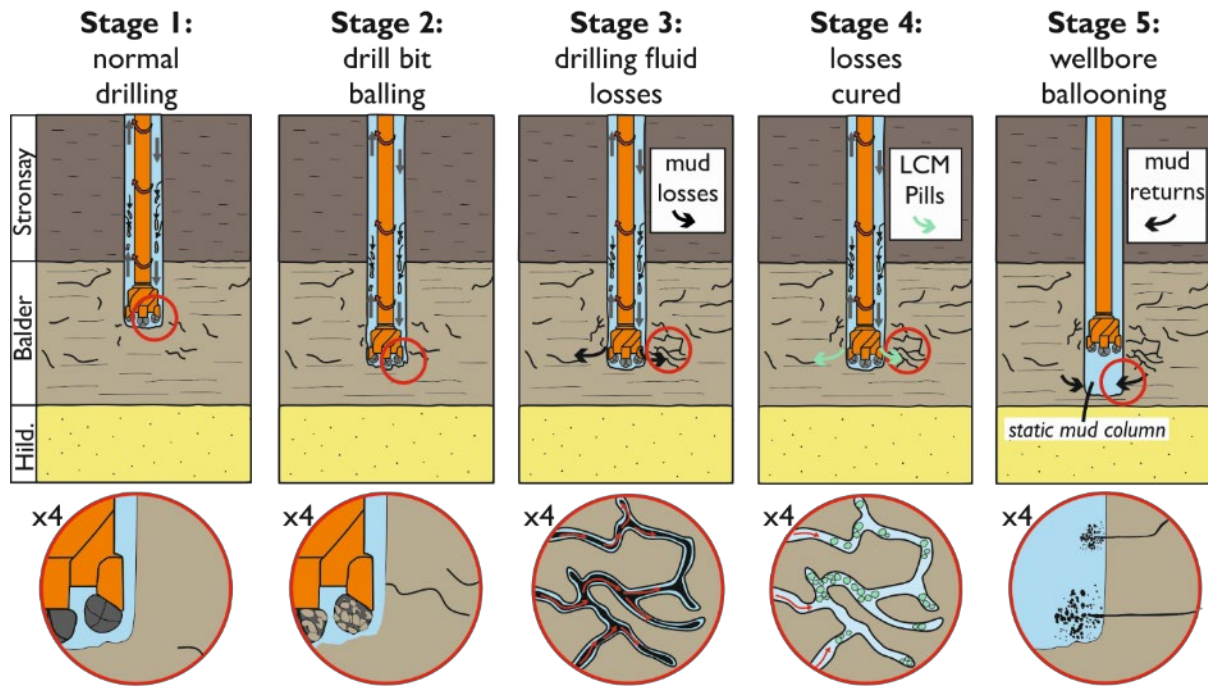


792

793 **Fig. 12.** Drilling window plot for well 213/26-1z with geomechanical explanation behind drilling
 794 induced fractures within the Balder Formation. The mud pressure (the ECD, in ppg) is not set

795 sufficiently high to induce fractures within the Balder Formation (i.e. it is below the regional Balder
 796 fracture pressure gradient). However, when the observed marked increase in standpipe pressure
 797 (called the *Excess Standpipe Pressure* in this plot) is combined with the ECD, then this pressure would
 798 exceed the anomalously low fracture pressure gradient of the Balder Formation around the Corona
 799 Ridge, at the exact depth where the losses occur.

800

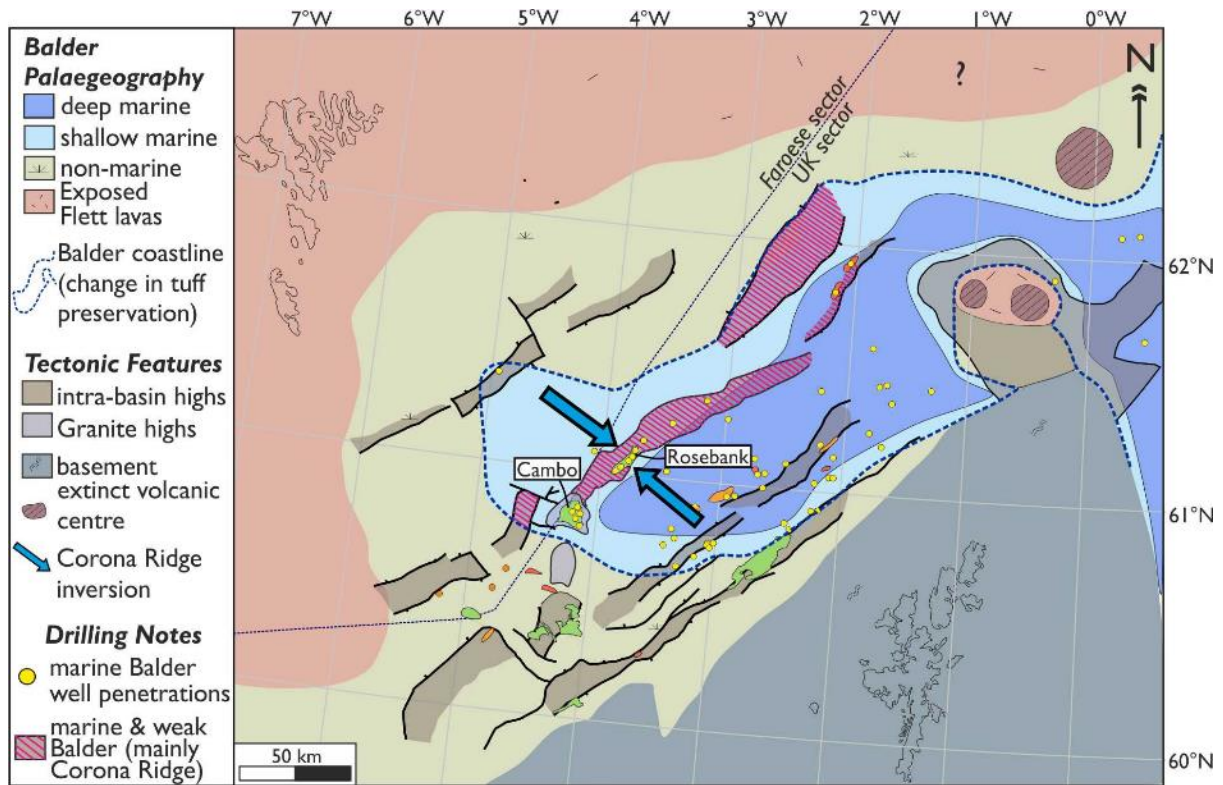


801

802

803 **Fig. 13.** Sequence of events leading to drilling issues encountered in the Balder Formation along the
 804 Corona Ridge. **Stage 1** represents normal drilling conditions, though by **Stage 2** the Balder
 805 Formation begins to react with drilling fluid and balls the drill bit, clogging the nozzles at the front of
 806 the bit, and leading to plugging of the wellbore above the bit and nozzles (a pack off), trapping pressure
 807 below. In **Stage 3** the trapped pressure below the pack-off causes the underlying formation to be
 808 subject to shock, causing pressures higher than measured and a drilling enhancement of natural
 809 fractures. Drilling fluid is lost to the fractures. These losses are cured (**Stage 4**), and drilling continues,
 810 though the drilling mud later returns to the wellbore (**Stage 5**), likely during connections (when more
 811 pipe is added to the drillstring) as the only thing holding back the formation fluids (including the drilling
 812 fluid lost earlier) is the pressure of the static mud column.

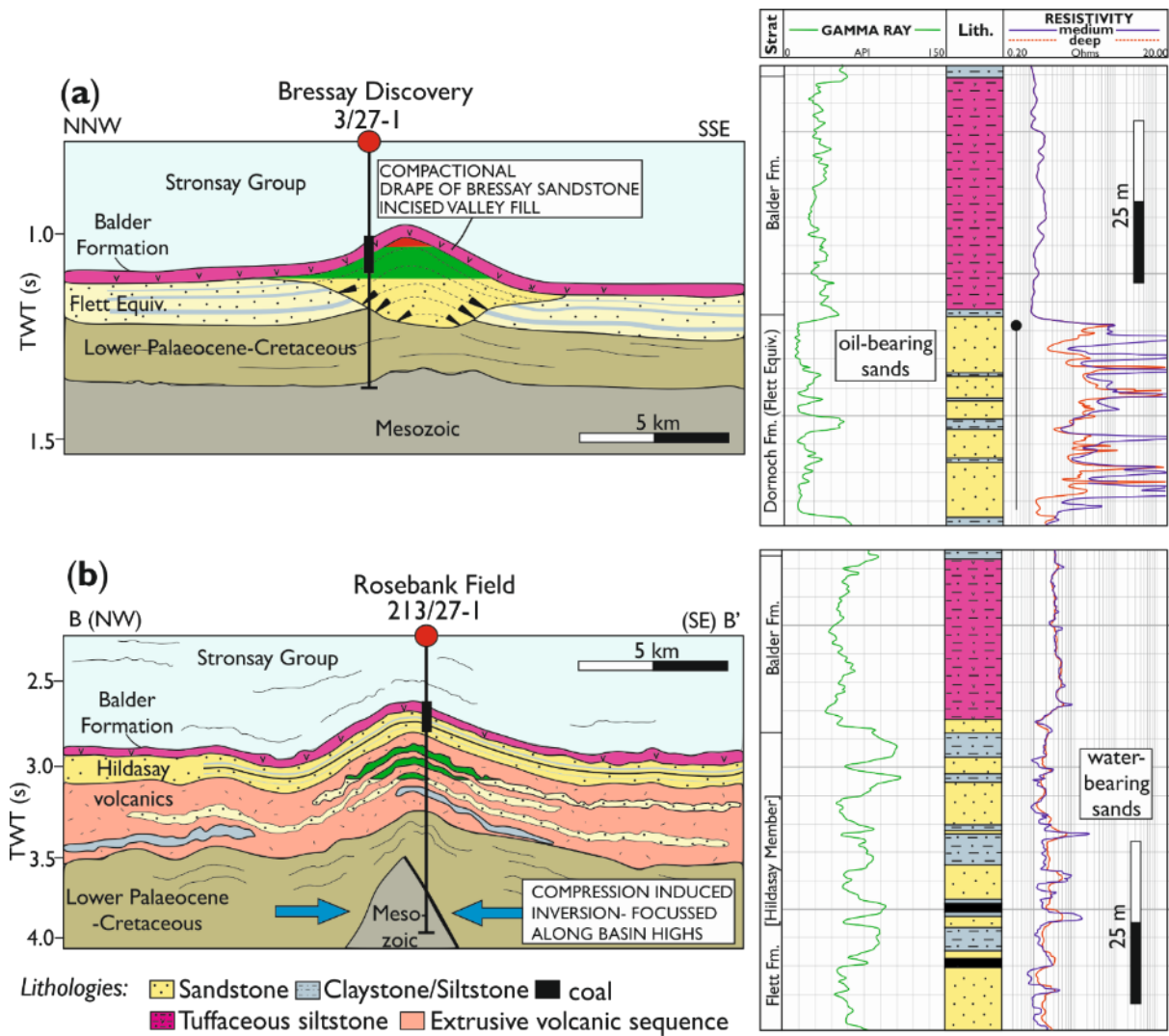
813



814

815 **Fig. 14.** Balder palaeogeography (adapted from Watson *et al.* 2017) showing areas of high risk of
 816 drilling issues through the Balder Formation (dashed red), corresponding to a marine setting overlying
 817 the Corona Ridge.

818



819

820

821 **Fig. 15.** Geoschematic comparison between the Bressay (a) and Rosebank (b) structures (location of
 822 Bressay and Rosebank displayed on Fig. 1). The Bressay structure formed as a result of differential
 823 compaction, with the Balder Formation acting as the top seal. In Rosebank, the structure formed
 824 tectonically due to regional compression, resulting in horizontal stresses that may have exceeded the
 825 fracture gradient of the Balder Formation. This fracture network, and associated permeability, would
 826 account for the water-bearing sandstones below the Balder Formation at Rosebank. Bressay cross-
 827 section adapted from Underhill (2001).
 828